université PARIS-SACLAY

ÉCOLE DOCTORALE
Sciences mécaniques et énergétiques, matériaux et géosciences (SMEMAG)

Piezoelectric fluid energy harvesters by monolithic fluid-structure-piezoelectric coupling: a full-scale finite element model

17-18 octobre 2024
Journées annuelles du GdR EX-MODELI | Lyon

Reporter — Runze ZHANG

Supervisor — A/Prof. Yu CONG

Content:

1 Research background

Recent work review

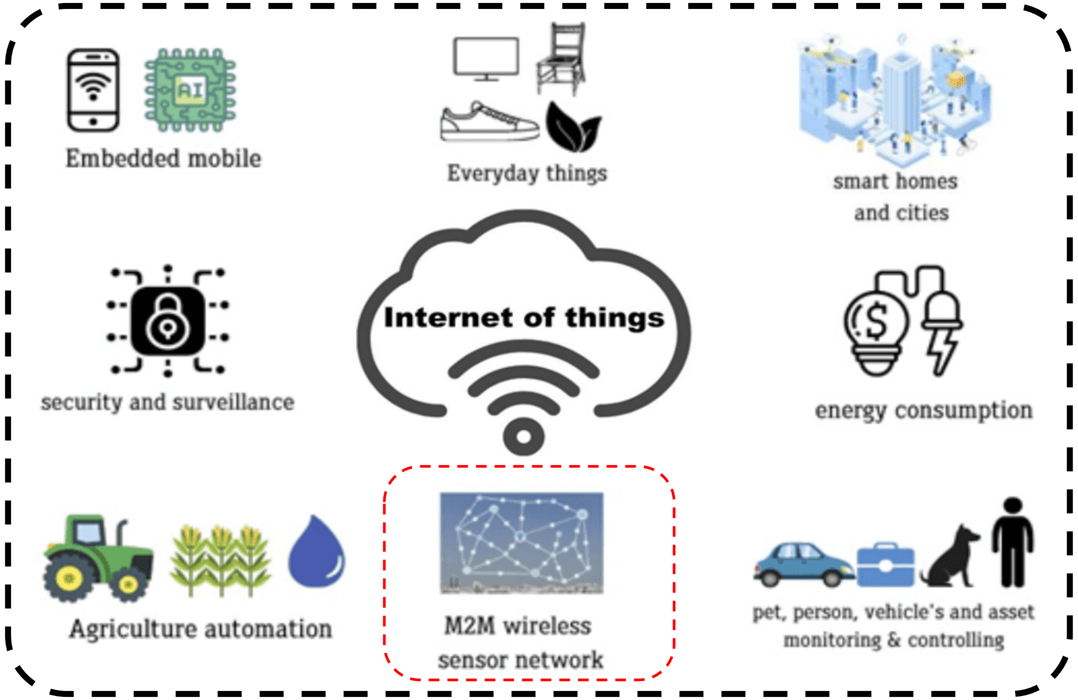

- The rise of the Internet of Things (IoT) has led to an increasing number of micro-electronic devices.
- These devices, including **wireless remote sensors**, are deployed in environments demanding extended lifespans and minimal maintenance.
- Consequently, there is a growing need to create reliable **self-powered systems** such as Piezoelectric fluid energy harvesters (PFEH) offering an alternative to traditional batteries.

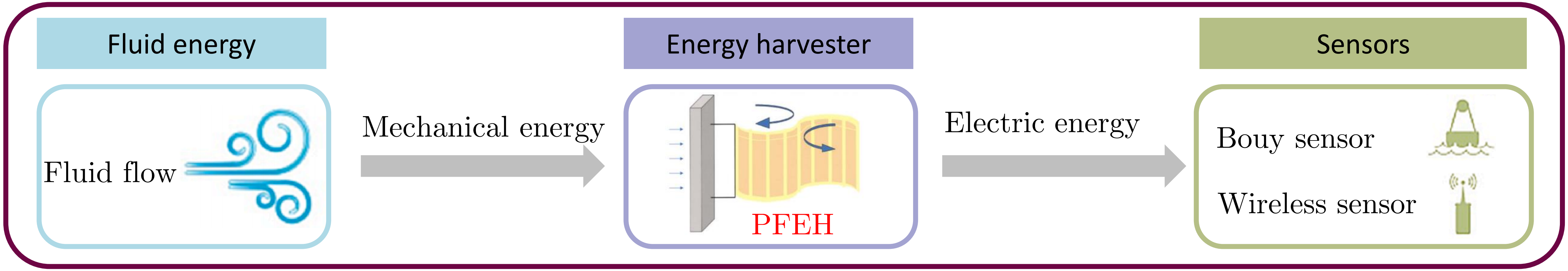

1 Research background

Recent work review

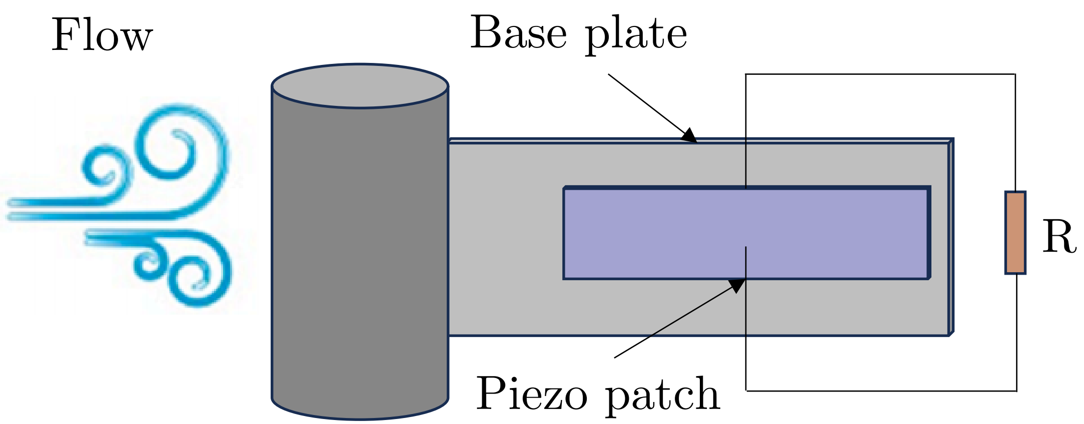

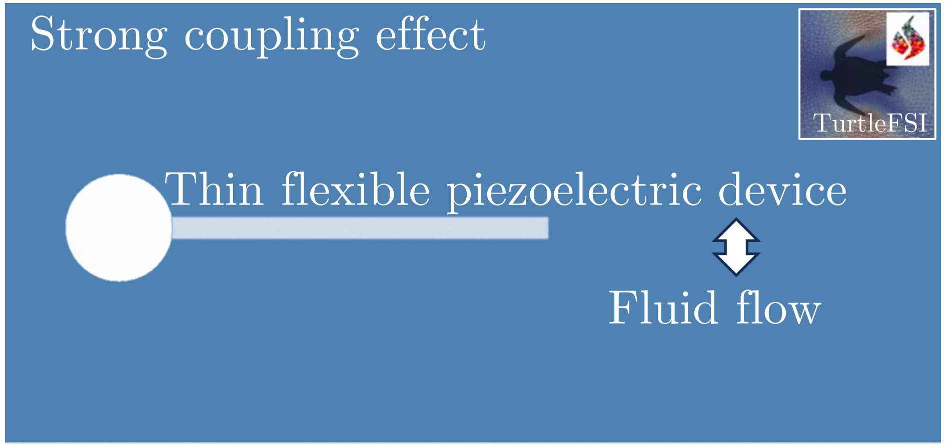

Recent research trend - complex PFEH designs

The choice for the structure model?

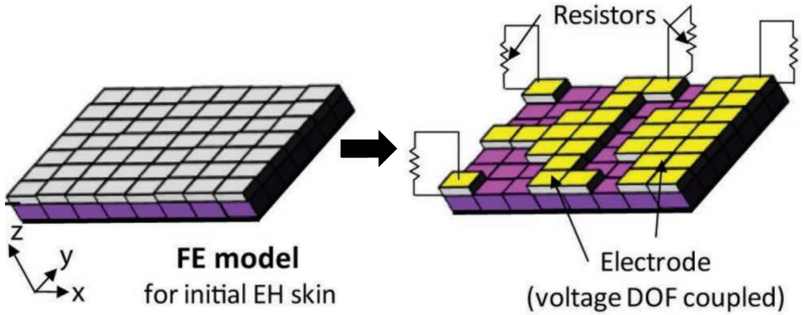

Fig. PEH topology optimization (Lee)

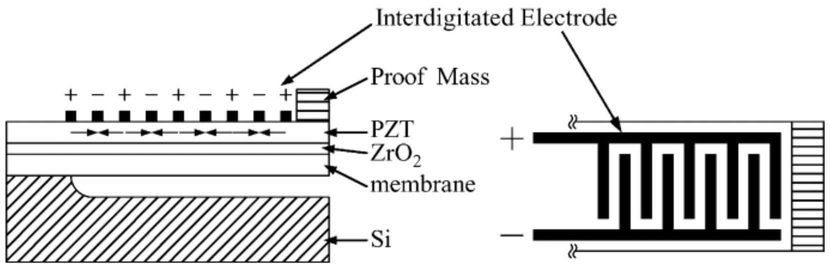

Fig. PEH electrode design (Jeon)

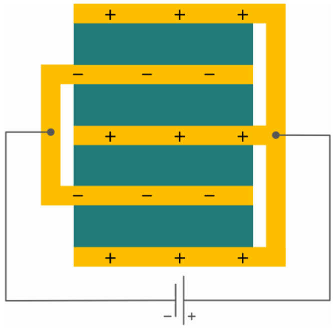

Fig. Stacked Configuration (Covaci)

- ➢ The **full-scale solid continuum** model outperforms simplified **beam/plate** models in complex PFEH designs.
- ➢ Especially in <u>micro-structured transducers</u> and <u>non-uniform cantilevers</u>, as well as the <u>induced local FSI effects</u>.

1 Research background

FSI coupling method

- Methods of solving coupled dynamic FSI problem are generally classified as **partitioned** and **monolithic** methods.

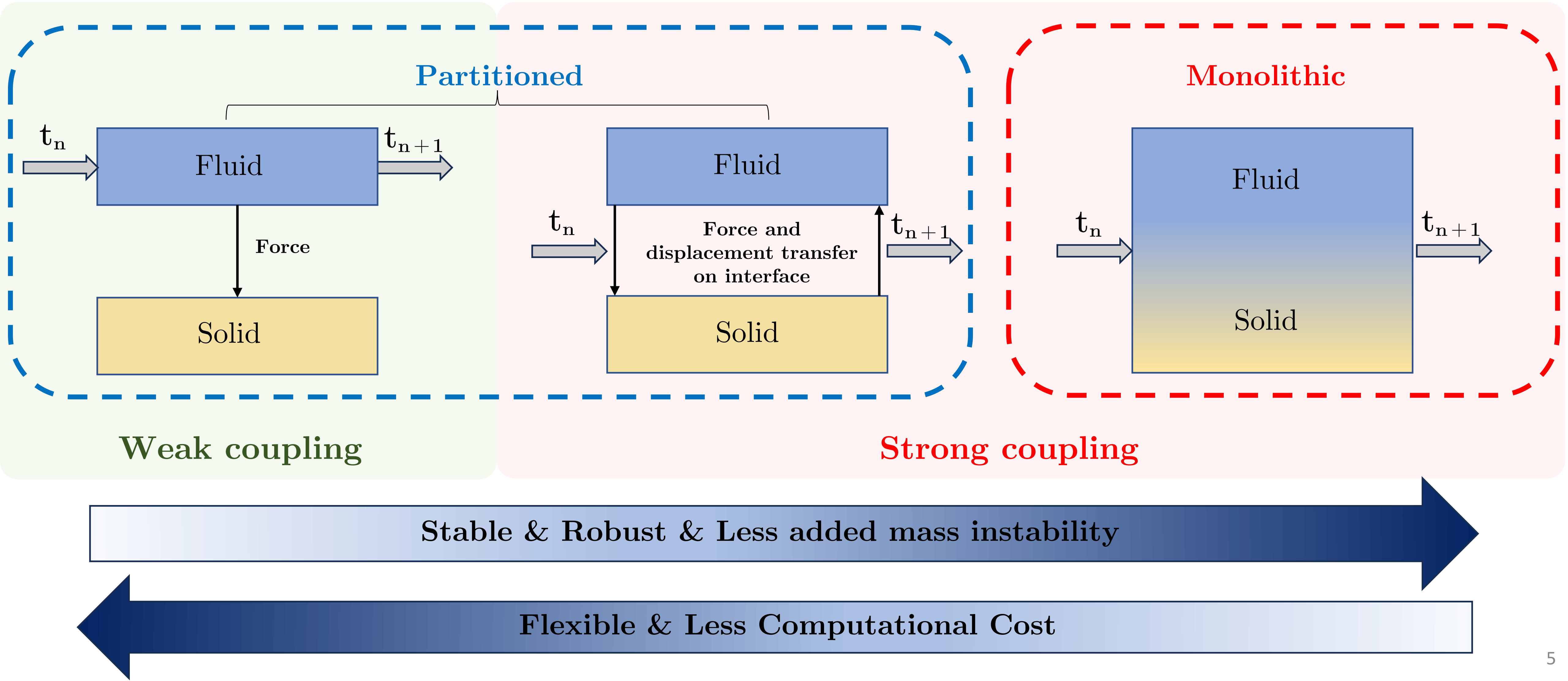

1 Research background

Research frame

A high-fidelity full-scale FEM model is built for monolithic FSI simulations of thin-walled PFEH

- **A solid continuum model with geometric nonlinearities is adopted.**

Complete coupling system

TurtleFSI

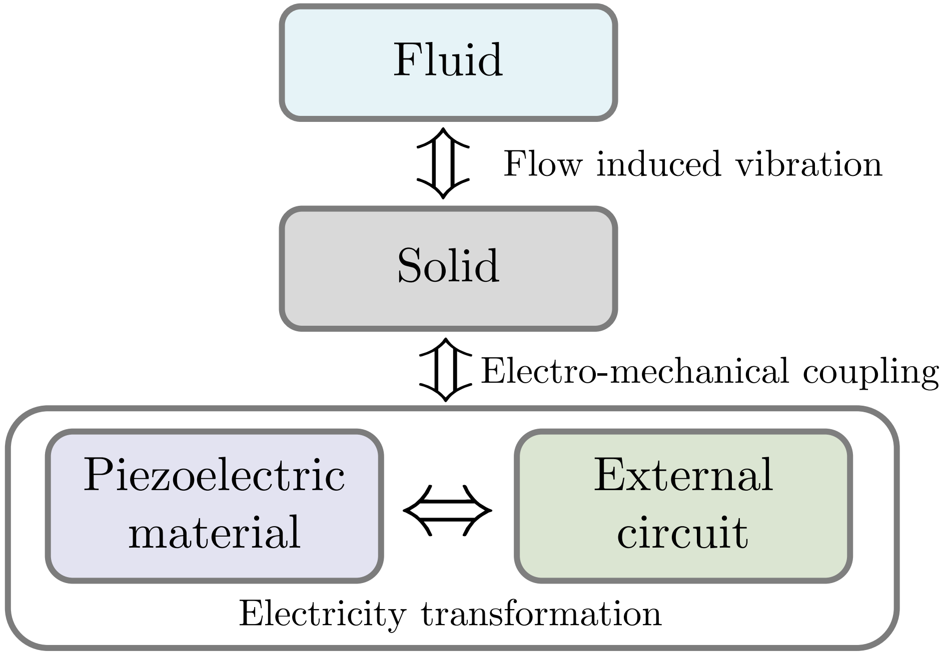

A set of numerical cases to demonstrate the solver's potential:

(1) Base plate cross-section shape

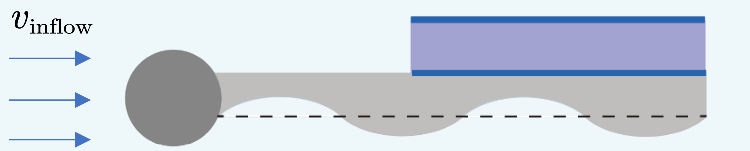

(2) Piezo patch location

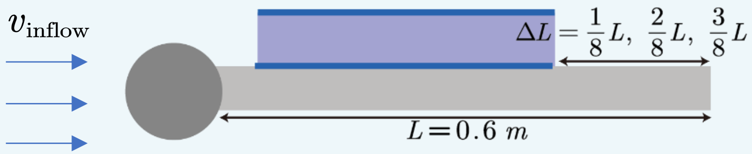

(3) Piezo patch inclusion

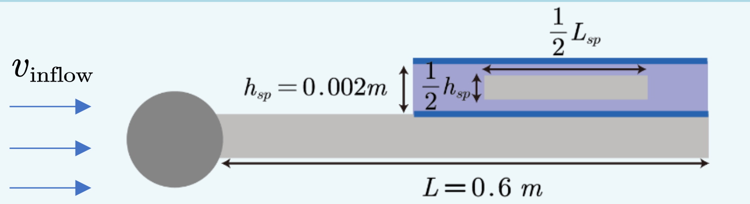

02 Governing equation

2. Governing equation

2.1 Strong form

Elastic solid domain

$$\rho_{ss}\partial_t^2\hat{\mathbf{u}}_{ss} - \hat{\nabla}\cdot\hat{\boldsymbol{\Pi}}_{ss} = 0, \quad \text{in } \hat{\Omega}_{ss} \quad \text{Newton's law}$$

$$\hat{\boldsymbol{\Pi}}_{ss} = \hat{\mathbf{F}}_{ss}\hat{\boldsymbol{\Sigma}}_{ss} = \hat{\mathbf{F}}_{ss}\mathbb{C}_{ss}:\hat{\mathbf{S}}_{ss}$$

$$\begin{cases} \hat{\mathbf{S}}_{ss} = 0.5\left(\hat{\mathbf{F}}_{ss}^{\mathrm{T}}\hat{\mathbf{F}}_{ss} - \mathbf{I}\right) \\ \hat{\mathbf{F}}_{ss} = \hat{\nabla}\hat{\mathbf{u}}_{ss} + \mathbf{I} \end{cases}$$

$\Leftrightarrow$

FSI Coupling Conditions

$$\hat{\mathbf{u}}_{\mathrm{A}} = \hat{\mathbf{u}}_{s}$$

$$\hat{\mathbf{v}}_{f} = \hat{\mathbf{v}}_{\mathrm{A}} = \partial_t\hat{\mathbf{u}}_{s} \quad \text{on } \hat{\Gamma}_{\mathrm{FSI}}$$

$$\left(\hat{\boldsymbol{J}}_{\mathrm{A}}\hat{\boldsymbol{\sigma}}_{f}\hat{\mathbf{F}}_{\mathrm{A}}^{-\mathrm{T}}\right)\cdot\hat{\mathbf{n}}_{\mathrm{FSI}} = \hat{\boldsymbol{\Pi}}_{s}\cdot\hat{\mathbf{n}}_{\mathrm{FSI}}$$

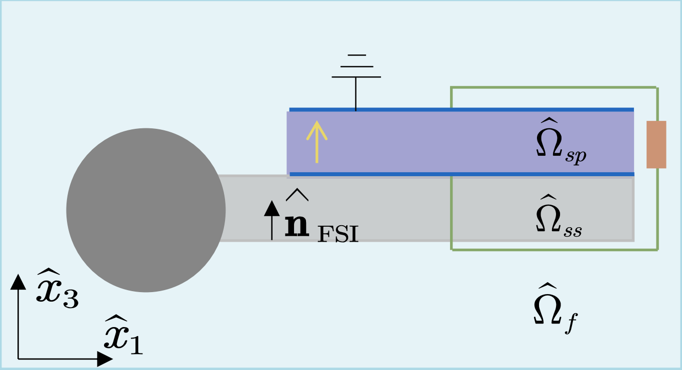

$\Updownarrow$

Piezoelectric solid domain

$$\begin{cases} \rho_{sp}\partial_t^2\hat{\mathbf{u}}_{sp} - \hat{\nabla}\cdot\hat{\boldsymbol{\Pi}}_{sp} = 0 \\ \hat{\nabla}\cdot\hat{\mathbf{D}}_{sp} = 0 \quad \text{Gauss equation} \end{cases}, \quad \text{in } \hat{\Omega}_{sp}$$

$$\begin{cases} \hat{\boldsymbol{\Pi}}_{sp} = \hat{\mathbf{F}}_{sp}\hat{\boldsymbol{\Sigma}}_{sp} = \hat{\mathbf{F}}_{sp}\left(\mathbb{C}:\hat{\mathbf{S}}_{sp} - \hat{\mathbf{e}}_{sp}\cdot\hat{\mathbf{E}}_{sp}\right) \\ \hat{\mathbf{D}}_{sp} = \mathbf{e}_{sp}:\hat{\mathbf{S}}_{sp} + \boldsymbol{\epsilon}_{sp}\cdot\hat{\mathbf{E}}_{sp} \end{cases}$$

$$\begin{cases} \hat{\mathbf{S}}_{sp} = 0.5\left(\hat{\mathbf{F}}_{sp}^{\mathrm{T}}\hat{\mathbf{F}}_{sp} - \mathbf{I}\right) \\ \hat{\mathbf{F}}_{sp} = \hat{\nabla}\hat{\boldsymbol{u}}_{sp} + \mathbf{I} \\ \hat{\mathbf{E}}_{sp} = -\hat{\nabla}\hat{\boldsymbol{\varphi}}_{sp} \end{cases}$$

Circuit

$$\hat{\boldsymbol{\varphi}}_{sp} = RI$$

$$I = \partial_t Q$$

Fluid domain in ALE framework

$$\begin{cases} \rho_f\hat{\boldsymbol{J}}_{\mathrm{A}}\partial_t\hat{\mathbf{v}}_f + \rho_f\hat{\boldsymbol{J}}_{\mathrm{A}}\hat{\mathbf{F}}_{\mathrm{A}}^{-1}\left(\hat{\mathbf{v}}_f - \partial_t\hat{\mathbf{u}}_{\mathrm{A}}\right)\cdot\hat{\mathbf{v}}_f - \hat{\nabla}\cdot\left(\hat{\boldsymbol{J}}_{\mathrm{A}}\hat{\boldsymbol{\sigma}}_f\hat{\mathbf{F}}_{\mathrm{A}}^{-\mathrm{T}}\right) = 0 \\ \hat{\nabla}\cdot\left(\hat{\boldsymbol{J}}_{\mathrm{A}}\hat{\mathbf{F}}_{\mathrm{A}}^{-1}\hat{\mathbf{v}}_f\right) = 0 \end{cases}, \quad \text{in } \hat{\Omega}_f$$

$$\hat{\boldsymbol{\sigma}}_f = -\hat{p}\mathbf{I} + 2\mu_f\hat{\boldsymbol{\varepsilon}}_f$$

$$\begin{cases} \hat{\boldsymbol{\varepsilon}}_f = 0.5\left(\left(\hat{\nabla}\hat{\mathbf{v}}_f\right)\hat{\mathbf{F}}_{\mathrm{A}}^{-1} + \hat{\mathbf{F}}_{\mathrm{A}}^{-\mathrm{T}}\left(\hat{\nabla}\hat{\mathbf{v}}_f\right)^{\mathrm{T}}\right) \\ \hat{\mathbf{F}}_{\mathrm{A}} = \hat{\nabla}\hat{\mathbf{u}}_{\mathrm{A}} + \mathbf{I} \end{cases}$$

Biharmonic mesh model

$$\hat{\boldsymbol{\eta}}_{\mathrm{A}} = -\alpha_u\hat{\Delta}\hat{\mathbf{u}}_{\mathrm{A}} \text{ and } -\alpha_u\hat{\Delta}\hat{\boldsymbol{\eta}}_{\mathrm{A}} = 0, \quad \text{in } \hat{\Omega}_f \qquad \alpha_u = 0.01$$

2. Governing equation

2.2 Weak form

Elastic solid domain

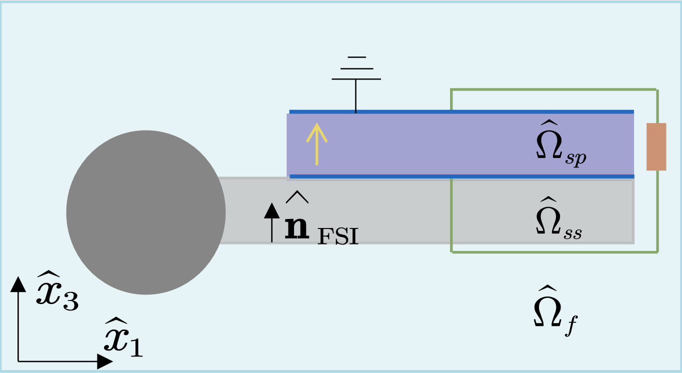

$$\int_{\hat{\Omega}_{ss}} \left(\rho_{ss}\partial_t \hat{\mathbf{v}}_{ss}\delta\hat{\mathbf{v}} + \widehat{\boldsymbol{\Pi}}_{ss}\hat{\nabla}\delta\hat{\mathbf{v}}\right) \mathrm{d}\hat{\Omega}_{ss} + \int_{\hat{\Gamma}_{\mathrm{FSI}}}\left(\widehat{\boldsymbol{\Pi}}_{ss}\cdot\hat{\mathbf{n}}_{\mathrm{FSI}}\delta\hat{\mathbf{v}}\right) \mathrm{d}\hat{\Omega}_{ss} = 0$$

Relate the displacement to velocity $\int_{\hat{\Omega}_{ss}} \rho_{ss}\left(\partial_t\hat{\mathbf{u}}_{ss} - \hat{\mathbf{v}}_{ss}\right)\delta\hat{\mathbf{u}}\ \mathrm{d}\hat{\Omega}_{ss} = 0$

Piezoelectric solid domain

$$\int_{\hat{\Omega}_{sp}} \left(\rho_{sp}\partial_t \hat{\mathbf{v}}_{sp}\delta\hat{\mathbf{v}} + \widehat{\boldsymbol{\Pi}}_{sp}\hat{\nabla}\delta\hat{\mathbf{v}}\right) \mathrm{d}\hat{\Omega}_{sp} + \int_{\hat{\Gamma}_{\mathrm{FSI}}}\left(\widehat{\boldsymbol{\Pi}}_{sp}\cdot\hat{\mathbf{n}}_{\mathrm{FSI}}\delta\hat{\mathbf{v}}\right) \mathrm{d}\hat{\Omega}_{sp} = 0$$

$$-\int_{\hat{\Omega}_{sp}} \hat{\mathbf{D}}_{sp}\left[\hat{\mathbf{E}}_{sp}\left(\delta\hat{\phi}\right)\right]\mathrm{d}\hat{\Omega}_{sp} + \underbrace{\int_{\hat{\Gamma}_{\mathrm{E}}}\left(-\frac{\Delta t}{R\,\mathrm{A}}\hat{\varphi} + \frac{Q^{t_n}}{\mathrm{A}}\right)\delta\hat{\phi}\,\mathrm{d}\hat{\Gamma}_{\mathrm{E}}}_{\text{Output circuit}} + \underbrace{\int_{\hat{\Gamma}_{\mathrm{E}}} 10^7\,\hat{\mathbf{E}}_{sp\,x_1}\left[\hat{\mathbf{D}}_{sp\,x_1}\left(\delta\hat{\mathbf{v}},\delta\hat{\phi}\right)\right]\mathrm{d}\hat{\Gamma}_{\mathrm{E}}}_{\text{Electrode boundary}} = 0$$

Relate $\hat{\mathbf{u}}$ to $\hat{\mathbf{v}}$ and $\hat{\varphi}$ to $\hat{\phi}$

$$\int_{\hat{\Omega}_{sp}} \rho_{sp}\left(\partial_t\hat{\mathbf{u}}_{sp} - \hat{\mathbf{v}}_{sp}\right)\delta\hat{\mathbf{u}}\ \mathrm{d}\hat{\Omega}_{sp} = 0$$

$$\int_{\hat{\Omega}_{sp}} \left(\partial_t\hat{\varphi} - \hat{\phi}\right)\delta\hat{\varphi}\ \mathrm{d}\hat{\Omega}_{sp} = 0$$

Fluid domain in ALE framework

$$\int_{\hat{\Omega}_f} \rho_f\hat{J}_{\mathrm{A}}\partial_t\hat{\mathbf{v}}_f\delta\hat{\mathbf{v}}\ \mathrm{d}\hat{\Omega}_f + \int_{\hat{\Omega}_f} \rho_f\hat{J}_{\mathrm{A}}\hat{\mathbf{F}}_{\mathrm{A}}^{-1}\left(\hat{\mathbf{v}}_f - \partial_t\hat{\mathbf{u}}_{\mathrm{A}}\right)\cdot\hat{\nabla}\hat{\mathbf{v}}_f\delta\hat{\mathbf{v}}\ \mathrm{d}\hat{\Omega}_f + \int_{\hat{\Omega}_f}\hat{\nabla}\cdot\left(\hat{J}_{\mathrm{A}}\hat{\boldsymbol{\sigma}}_f\hat{\mathbf{F}}_{\mathrm{A}}^{-\mathrm{T}}\right)\delta\hat{\mathbf{v}}\ \mathrm{d}\hat{\Omega}_f - \int_{\hat{\Gamma}_{\mathrm{FSI}}}\left(\hat{J}_{\mathrm{A}}\hat{\boldsymbol{\sigma}}_f\hat{\mathbf{F}}_{\mathrm{A}}^{-\mathrm{T}}\right)\cdot\hat{\mathbf{n}}_{\mathrm{FSI}}\delta\hat{\mathbf{v}}\ \mathrm{d}\hat{\Gamma}_{\mathrm{FSI}} = 0$$

$$\int_{\hat{\Omega}_f}\hat{\nabla}\cdot\left(\hat{J}_{\mathrm{A}}\hat{\mathbf{F}}_{\mathrm{A}}^{-1}\hat{\mathbf{v}}_f\right)\delta\hat{p}\ \mathrm{d}\hat{\Omega}_f$$

Biharmonic mesh model $\int_{\hat{\Omega}_f}\left(\hat{\boldsymbol{\eta}}_{\mathrm{A}} - \alpha_u\hat{\nabla}\hat{\mathbf{u}}_{\mathrm{A}}\right)\delta\hat{\boldsymbol{\eta}}\ \mathrm{d}\hat{\Omega}_f$ and $\int_{\hat{\Omega}_f}\alpha_u\hat{\nabla}\hat{\boldsymbol{\eta}}_{\mathrm{A}}\hat{\nabla}\delta\hat{\mathbf{u}}\ \mathrm{d}\hat{\Omega}_f$

2. Governing equation

2.3 Time integration

One step θ method

The temporal discretization is achieved by using an implicit one-step θ method.

Considering a generic equation ($\boldsymbol{a}$: generic variable), the one-step θ method amounts to solving for the time-step $n+1$

$$\left[\frac{\partial \boldsymbol{a}}{\partial t}+f(\boldsymbol{a})\right]^{n+1}=0 \quad \rightarrow \quad \frac{\boldsymbol{a}^{n+1}-\boldsymbol{a}^{n}}{\Delta t}+\theta[f(\boldsymbol{a})]^{n+1}+(1-\theta)[f(\boldsymbol{a})]^{n}=0$$

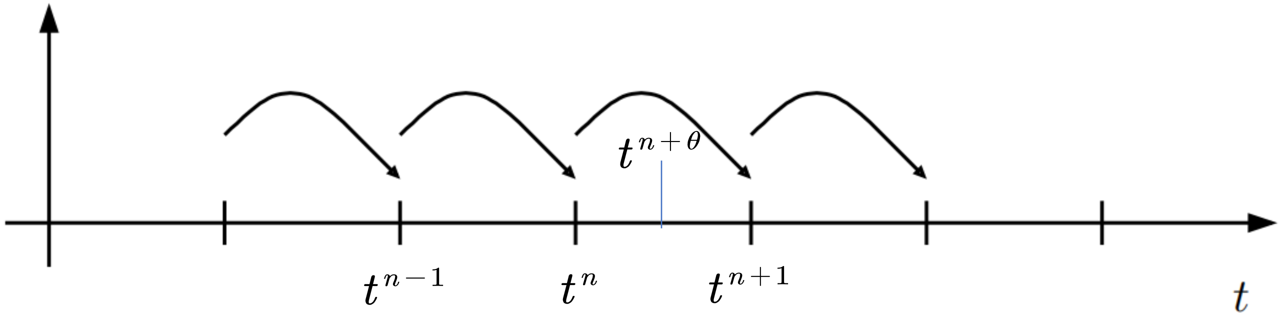

Different numerical stability and time accuracy for different ϑ

$$\begin{cases} \theta=1 & \textbf{\textit{Euler scheme}}\text{: unconditional stable in a stationary solver; first order time accuracy} \\ \theta=1/2 & \textbf{\textit{Crank}}-\textbf{\textit{Nicholson scheme}}\text{: numerical instabilities in dynamic fsi; second order time accuracy} \\ \theta=1/2+\Delta t & \textbf{\textit{shifted Crank}}-\textbf{\textit{Nicholson scheme}}\text{: stable in dynamic fsi; first order time accuracy} \end{cases}$$

For better robustness, shifted Crank Nicholson scheme is adopted.

2. Governing equation

2.3 Time integration

One step θ method

Fluid part

Temporal derivative $$+\int_{\hat\Omega_f}\theta_0\rho_f\left[\hat{\boldsymbol{J}}_{\mathrm{A}}\left(\hat{\mathbf{u}}_n\right)\right]\frac{\left(\hat{\mathbf{v}}_n-\hat{\mathbf{v}}_{n-1}\right)}{\Delta t}\delta\hat{\mathbf{v}}\;\mathrm{d}\hat\Omega_f+\int_{\hat\Omega_f}\theta_1\rho_f\left[\hat{\boldsymbol{J}}_{\mathrm{A}}\left(\hat{\mathbf{u}}_{n-1}\right)\right]\frac{\left(\hat{\mathbf{v}}_n-\hat{\mathbf{v}}_{n-1}\right)}{\Delta t}\delta\hat{\mathbf{v}}\;\mathrm{d}\hat\Omega_f$$

Convection $$+\int_{\hat\Omega_f}\theta_0\rho_f\left[\hat{\boldsymbol{J}}_{\mathrm{A}}\left(\hat{\mathbf{u}}_n\right)\right]\left[\hat{\mathbf{F}}_{\mathrm{A}}\left(\hat{\mathbf{u}}_n\right)\right]^{-1}\hat{\mathbf{v}}_n\cdot\left[\hat\nabla\left(\hat{\mathbf{v}}_n\right)\right]\delta\hat{\mathbf{v}}\;\mathrm{d}\hat\Omega_f+\int_{\hat\Omega_f}\theta_1\rho_f\left[\hat{\boldsymbol{J}}_{\mathrm{A}}\left(\hat{\mathbf{u}}_{n-1}\right)\right]\left[\hat{\mathbf{F}}_{\mathrm{A}}\left(\hat{\mathbf{u}}_{n-1}\right)\right]^{-1}\hat{\mathbf{v}}_{n-1}\cdot\left[\hat\nabla\left(\hat{\mathbf{v}}_{n-1}\right)\right]\delta\hat{\mathbf{v}}\;\mathrm{d}\hat\Omega_f$$

ALE term $$-\int_{\hat\Omega_f}\rho_f\left[\hat{\boldsymbol{J}}_{\mathrm{A}}\left(\hat{\mathbf{u}}_n\right)\right]\left[\hat{\mathbf{F}}_{\mathrm{A}}\left(\hat{\mathbf{u}}_n\right)\right]^{-1}\frac{\left(\hat{\mathbf{u}}_n-\hat{\mathbf{u}}_{n-1}\right)}{\Delta t}\cdot\left[\hat\nabla\left(\hat{\mathbf{v}}_n\right)\right]\delta\hat{\mathbf{v}}\;\mathrm{d}\hat\Omega_f$$

$$\hat{\boldsymbol{\sigma}}_f=\hat{\boldsymbol{\sigma}}_{fp}+\hat{\boldsymbol{\sigma}}_{fu}$$
$$=-\hat{p}\mathbf{I}+2\mu_f\hat{\boldsymbol{\varepsilon}}_f$$

Stress from pressure $$+\int_{\hat\Omega_f}\left[\hat{\boldsymbol{J}}_{\mathrm{A}}\left(\hat{\mathbf{u}}_n\right)\right]\left[\hat{\boldsymbol{\sigma}}_{fp}\left(\hat{p}_n\right)\right]\left[\hat{\mathbf{F}}_{\mathrm{A}}\left(\hat{\mathbf{u}}_n\right)\right]^{-\mathrm{T}}\hat\nabla\left(\delta\hat{\mathbf{v}}\right)\;\mathrm{d}\hat\Omega_f$$

Stress from velocity $$+\int_{\hat\Omega_f}\theta_0\left[\hat{\boldsymbol{J}}_{\mathrm{A}}\left(\hat{\mathbf{u}}_n\right)\right]\left[\hat{\boldsymbol{\sigma}}_{fu}\left(\hat{\mathbf{v}}_n,\hat{\mathbf{u}}_n\right)\right]\left[\hat{\mathbf{F}}_{\mathrm{A}}\left(\hat{\mathbf{u}}_n\right)\right]^{-\mathrm{T}}\hat\nabla\left(\delta\hat{\mathbf{v}}\right)\;\mathrm{d}\hat\Omega_f+\int_{\hat\Omega_f}\theta_1\left[\hat{\boldsymbol{J}}_{\mathrm{A}}\left(\hat{\mathbf{u}}_{n-1}\right)\right]\left[\sigma_{fu}\left(\hat{\mathbf{v}}_{n-1},\hat{\mathbf{u}}_{n-1}\right)\right]\left[\hat{\mathbf{F}}_{\mathrm{A}}\left(\hat{\mathbf{u}}_{n-1}\right)\right]^{-\mathrm{T}}\hat\nabla\left(\delta\hat{\mathbf{v}}\right)\;\mathrm{d}\hat\Omega_f$$

Divergence free term $$+\int_{\hat\Omega_f}\left\{\nabla\cdot\left[\hat{\boldsymbol{J}}_{\mathrm{A}}\left(\hat{\mathbf{u}}_n\right)\right]\left[\hat{\mathbf{F}}_{\mathrm{A}}\left(\hat{\mathbf{u}}_n\right)\right]^{-1}\hat{\mathbf{v}}_n\right\}\delta\hat{p}\;\mathrm{d}\hat\Omega_f$$

Biharmonic Mesh operator $$+\int_{\hat\Omega_f}\alpha_{\mathrm{u}}\hat{\boldsymbol{\eta}}_n\cdot\delta\hat{\boldsymbol{\eta}}\;\mathrm{d}\hat\Omega_f-\int_{\hat\Omega_f}\alpha_{\mathrm{u}}\hat\nabla\hat{\mathbf{u}}_n:\hat\nabla\delta\hat{\boldsymbol{\eta}}\;\mathrm{d}\hat\Omega_f$$

Biharmonic Mesh operator $$+\int_{\hat\Omega_f}\alpha_{\mathrm{u}}\hat\nabla\hat{\boldsymbol{\eta}}_n:\hat\nabla\delta\hat{\mathbf{u}}\;\mathrm{d}\hat\Omega_f=0$$

2. Governing equation

2.3 Time integration

One step θ method

Elastic Solid part

$$\begin{cases} \theta_1 = 1-\theta \\ \theta_0 = \theta \end{cases}$$

Temporal term $$+\int_{\hat\Omega_{ss}} \rho_{ss} \frac{\left(\hat{\mathbf v}_n - \hat{\mathbf v}_{n-1}\right)}{\Delta t} \cdot \delta\hat{\mathbf v}\; d\hat\Omega_{ss}$$

Stress $$+\int_{\hat\Omega_{ss}} \theta_1 \widehat{\boldsymbol\Pi}_{ss}\left(\hat{\mathbf u}_{n-1}\right) : \hat\nabla\left(\delta\hat{\mathbf v}\right) d\hat\Omega_{ss} + \int_{\hat\Omega_{ss}} \theta_0 \widehat{\boldsymbol\Pi}_{ss}\left(\hat{\mathbf u}_{n}\right) : \hat\nabla\left(\delta\hat{\mathbf v}\right) d\hat\Omega_{ss}$$

Convection term $$+\int_{\hat\Omega_{ss}} \rho_{ss} \left[\frac{\left(\hat{\mathbf u}_n - \hat{\mathbf u}_{n-1}\right)}{\Delta t} - \left(\theta_0 \hat{\mathbf v}_n + \theta_1 \hat{\mathbf v}_{n-1}\right)\right] \cdot \delta\hat{\mathbf u}\; d\hat\Omega_{ss} = 0$$

Piezo Solid part

$$+\int_{\hat\Omega_{sp}} \rho_{sp} \frac{\left(\hat{\mathbf v}_n - \hat{\mathbf v}_{n-1}\right)}{\Delta t} \cdot \delta\hat{\mathbf v}\; d\hat\Omega_{sp}$$

$$+\int_{\hat\Omega_{sp}} \theta_1 \widehat{\boldsymbol\Pi}_{sp}\left(\hat{\mathbf u}_{n-1}, \hat{\boldsymbol\varphi}_{n-1}\right) : \hat\nabla\left(\delta\hat{\mathbf v}\right) d\hat\Omega_{sp} + \int_{\hat\Omega_{sp}} \theta_0 \widehat{\boldsymbol\Pi}_{sp}\left(\hat{\mathbf u}_{n}, \hat{\boldsymbol\varphi}_{n}\right) : \hat\nabla\left(\delta\hat{\mathbf v}\right) d\hat\Omega_{sp}$$

$$-\int_{\hat\Omega_{sp}} \theta_1 \hat{\mathbf D}_{sp}\left(\hat{\mathbf u}_{n-1}, \boldsymbol\varphi_{n-1}\right) : \hat{\mathbf E}_{sp}\left(\delta\hat{\boldsymbol\phi}\right) d\hat\Omega_{sp} - \int_{\hat\Omega_{sp}} \theta_0 \hat{\mathbf D}_{sp}\left(\hat{\mathbf u}_{n}, \hat{\boldsymbol\varphi}_{n}\right) : \hat{\mathbf E}_{sp}\left(\delta\hat{\boldsymbol\phi}\right) d\hat\Omega_{sp}$$

$$+10^7 \int_{\hat\Gamma_{\mathrm E}} \left[\theta_1 \hat{\mathbf E}_{sp\,x_1}\left(\hat{\boldsymbol\varphi}_{n-1}\right) \hat{\mathbf D}_{sp\,x_1}\left(\delta\hat{\mathbf v}, \delta\hat{\boldsymbol\phi}\right) + \theta_0 \hat{\mathbf E}_{sp\,x_1}\left(\hat{\boldsymbol\varphi}_{n}\right) \hat{\mathbf D}_{sp\,x_1}\left(\delta\hat{\mathbf v}, \delta\hat{\boldsymbol\phi}\right)\right] d\hat\Gamma_{\mathrm E}$$

Electrode term

$$+\int_{\hat\Gamma_{\mathrm E}} \left(-\frac{\Delta t}{R\,\mathrm A} \hat{\boldsymbol\varphi}_n + \frac{Q^{t_{n-1}}}{\mathrm A}\right) \delta\hat{\boldsymbol\phi}\, d\hat\Gamma_{\mathrm E}$$

Circuit term

$$+\int_{\hat\Omega_{sp}} \rho_{sp} \left[\frac{\left(\hat{\mathbf u}_n - \hat{\mathbf u}_{n-1}\right)}{\Delta t} - \left(\theta_0 \hat{\mathbf v}_n + \theta_1 \hat{\mathbf v}_{n-1}\right)\right] \cdot \delta\hat{\mathbf u}\; d\hat\Omega_{sp}$$

$$+\int_{\hat\Omega_{sp}} \left[\frac{\left(\hat{\boldsymbol\varphi}_n - \hat{\boldsymbol\varphi}_{n-1}\right)}{\Delta t} - \left(\theta_0 \hat{\boldsymbol\phi}_n + \theta_1 \hat{\boldsymbol\phi}_{n-1}\right)\right] \cdot \delta\hat{\boldsymbol\varphi}\; d\hat\Omega_{sp} = 0$$

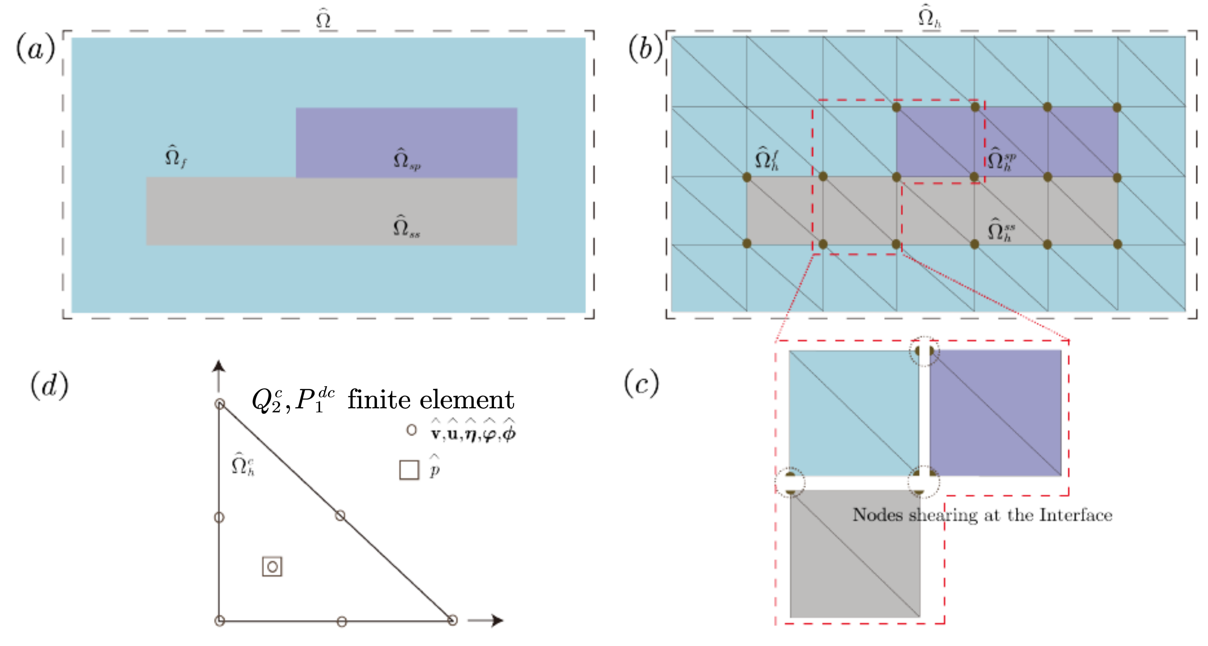

Monolithic computational mesh

03 Simulation results

Fluid-structure-piezoelectric coupling system with output circuit

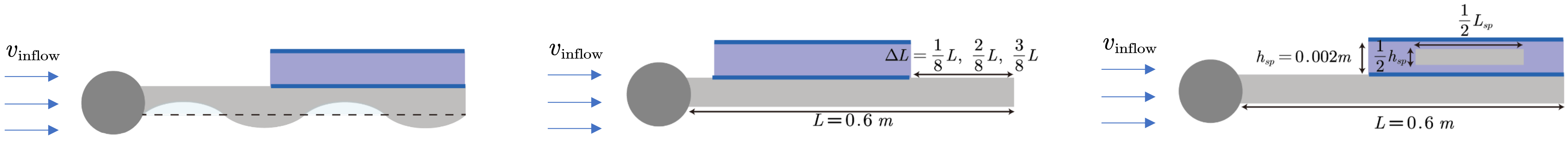

Three configurations

3. Simulation results

3.1 Standard case

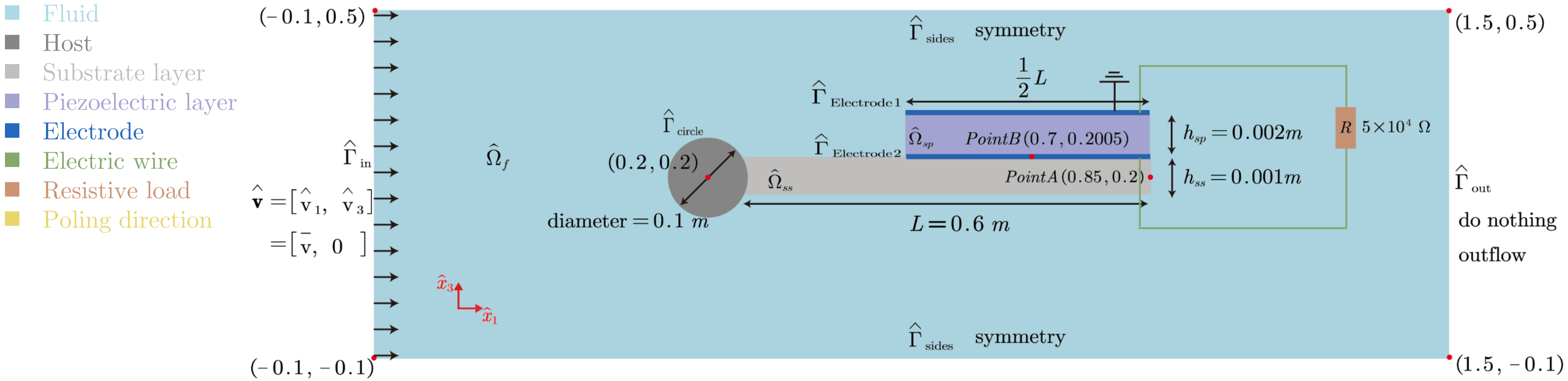

Fluid parameters in $\hat{\boldsymbol{\Omega}}_f$ (Glycerine)

$$\rho_f = 1200\ \text{kg/m}^3$$
$$\mu_f = 1.42\ \text{kg/ms}$$
$$\bar{v}_{inlet} = 2\ \text{m/s}$$
$$\text{Re} = 170$$

Mechanical parameters in $\hat{\boldsymbol{\Omega}}_{ss}$ (Aluminum alloy)

$$\rho_{ss} = 2800\ \text{kg/m}^3$$
$$c_{11} = 112\ \text{GPa}$$
$$c_{12} = 60.5\ \text{GPa}$$

Mechanical and electrical parameters in $\hat{\boldsymbol{\Omega}}_{sp}$ (PZT-5A)

$$\rho_{sp} = 7750\ \text{kg/m}^3$$
$$c_{11} = 120.35\ \text{GPa}$$
$$c_{13} = 75.09\ \text{GPa}$$
$$c_{33} = 110.9\ \text{GPa}$$
$$c_{44} = 21.05\ \text{GPa}$$
$$e_{15} = 12.29\ \text{C}\cdot\text{m}^{-2}$$
$$e_{31} = -5.35\ \text{C}\cdot\text{m}^{-2}$$
$$e_{33} = 15.78\ \text{C}\cdot\text{m}^{-2}$$
$$\epsilon_{11} = 8.14\times10^{-9}\ \text{C}\cdot\text{V}^{-1}$$
$$\epsilon_{33} = 7.32\times10^{-9}\ \text{C}\cdot\text{V}^{-1}$$
$$R = 5\times10^4\ \Omega$$

3. Simulation results

3.2 Cases changing Base plate shape

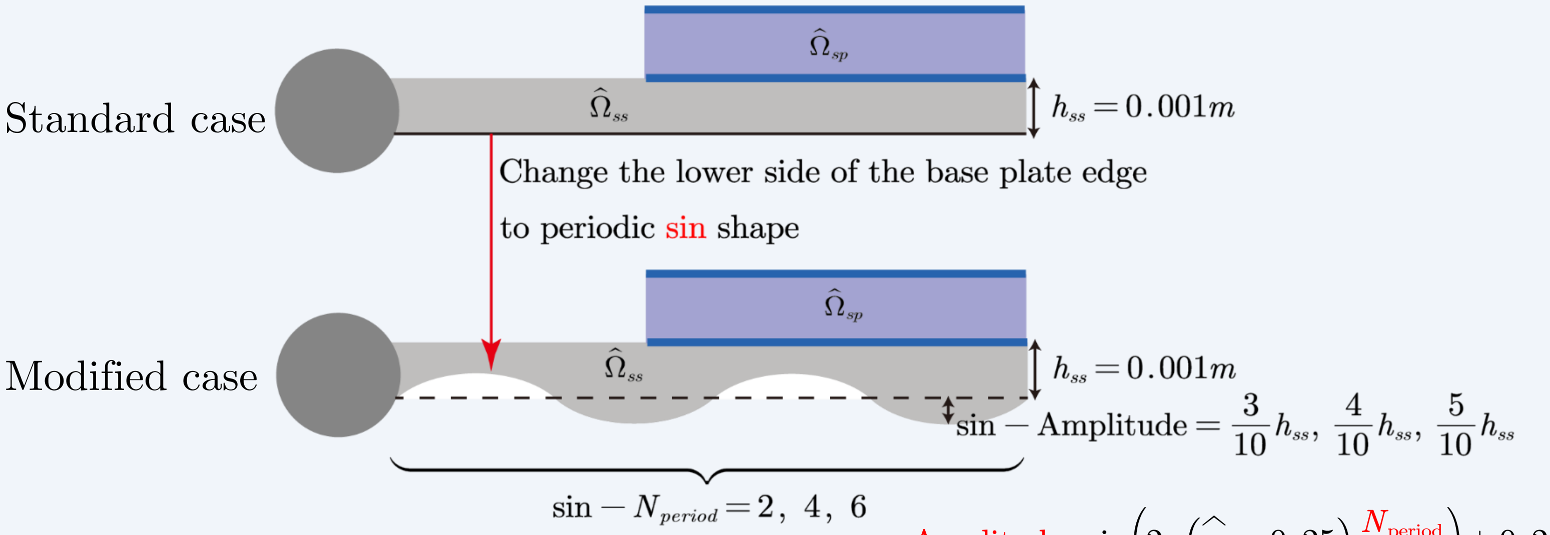

$$\text{Amplitude}\cdot\sin\left(2\pi\left(\widehat{x_1}-0.25\right)\frac{N_{\text{period}}}{L}\right)+0.2$$

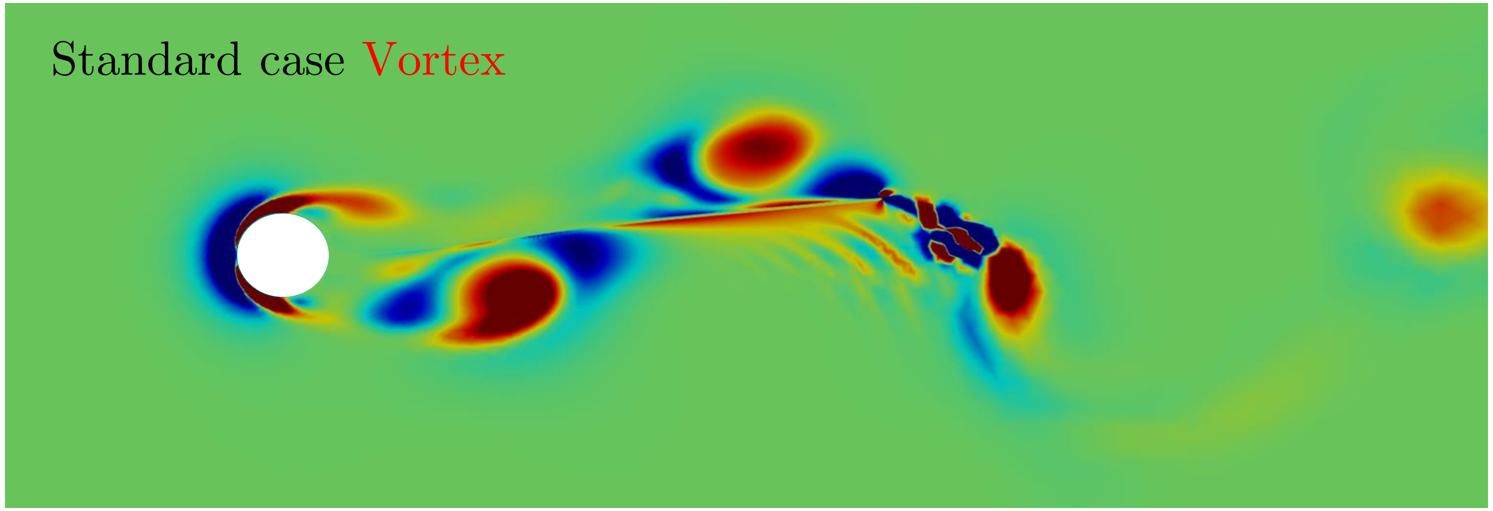

Cases settings

Case name	sin-Amplitude	sin-N_{period}
FSEI-(1)	/	/
FSEI-(2)	$3/10h_{ss}$	6
FSEI-(3)	$4/10h_{ss}$	6
FSEI-(4)	$5/10h_{ss}$	2
FSEI-(5)	$5/10h_{ss}$	4
FSEI-(6)	$5/10h_{ss}$	6

sin-Amplitude $\begin{cases}\text{FSEI-(1)}\\ \text{FSEI-(2)}\\ \text{FSEI-(3)}\\ \text{FSEI-(6)}\end{cases}$

sin-N_{period} $\begin{cases}\text{FSEI-(1)}\\ \text{FSEI-(4)}\\ \text{FSEI-(5)}\\ \text{FSEI-(6)}\end{cases}$

3. Simulation results

3.2 Cases changing Base plate shape: sin-Amplitude

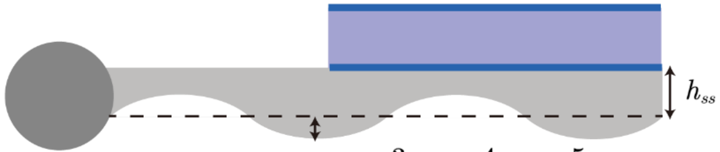

$\text{sin} - \text{Amplitude} = \frac{3}{10}h_{ss},\ \frac{4}{10}h_{ss},\ \frac{5}{10}h_{ss}$

$$\text{Efficiency} = \frac{\text{AveragedPower}}{0.5\rho \bar{v}^3 (2\hat{u}_{3,\max})}$$

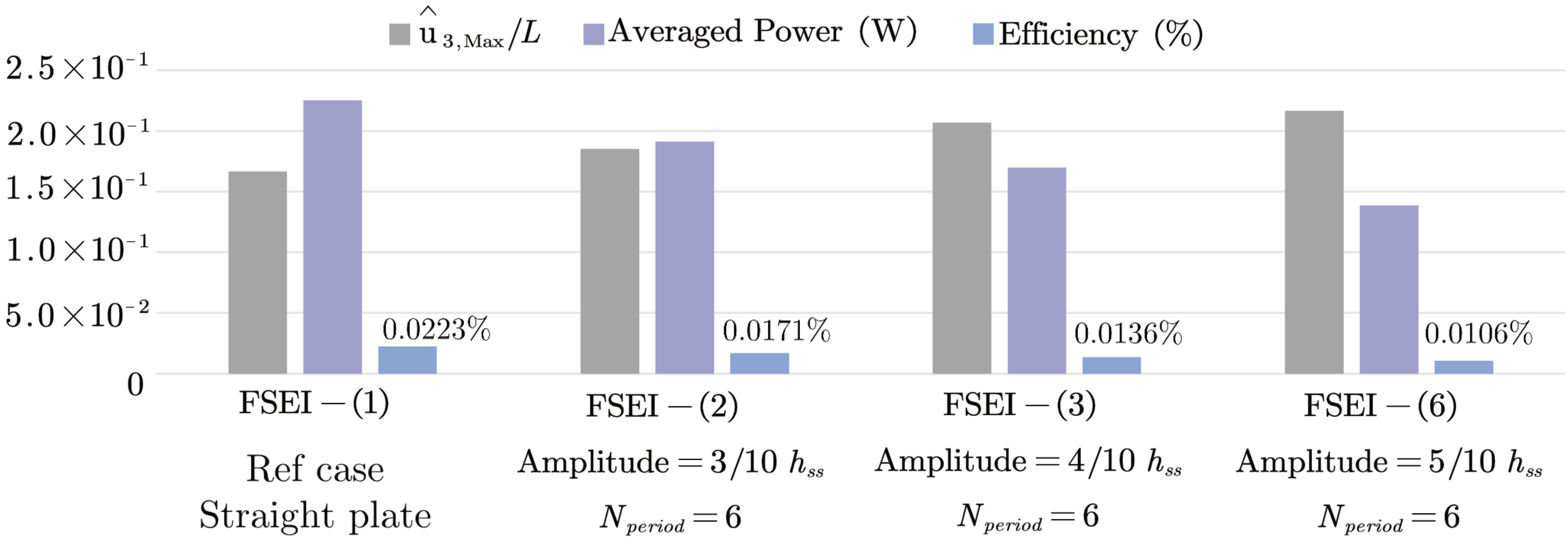

Statistic data extracted from Time history results

- ☐ The increase of sin-Amplitude will enlarge the free end displacement and decrease the output averaged power, then the corresponding energy harvesting efficiency will also decrease.

3. Simulation results

3.2 Cases changing Base plate shape: sin-N_{period}

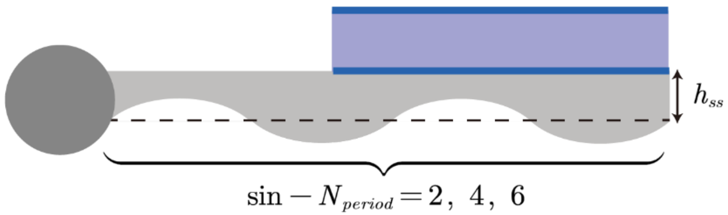

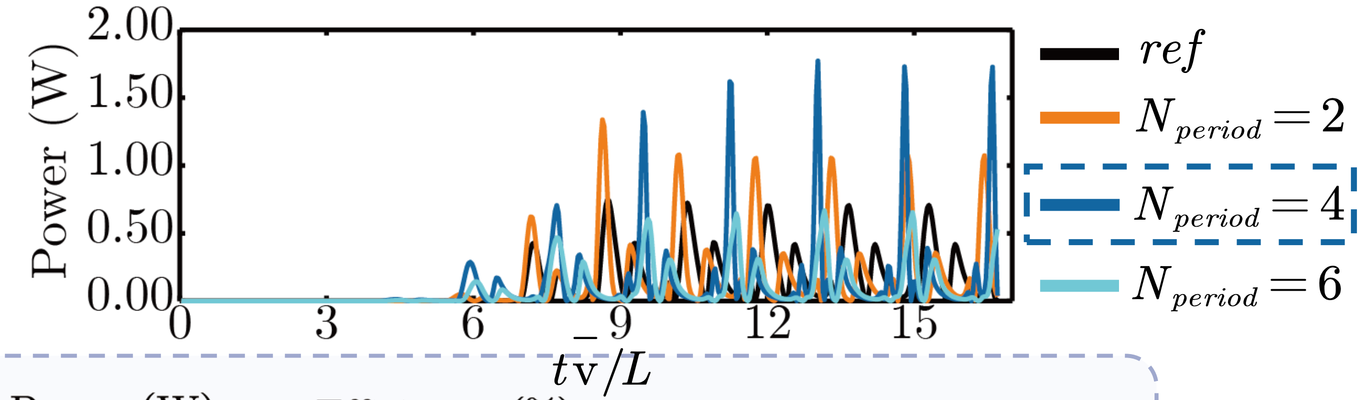

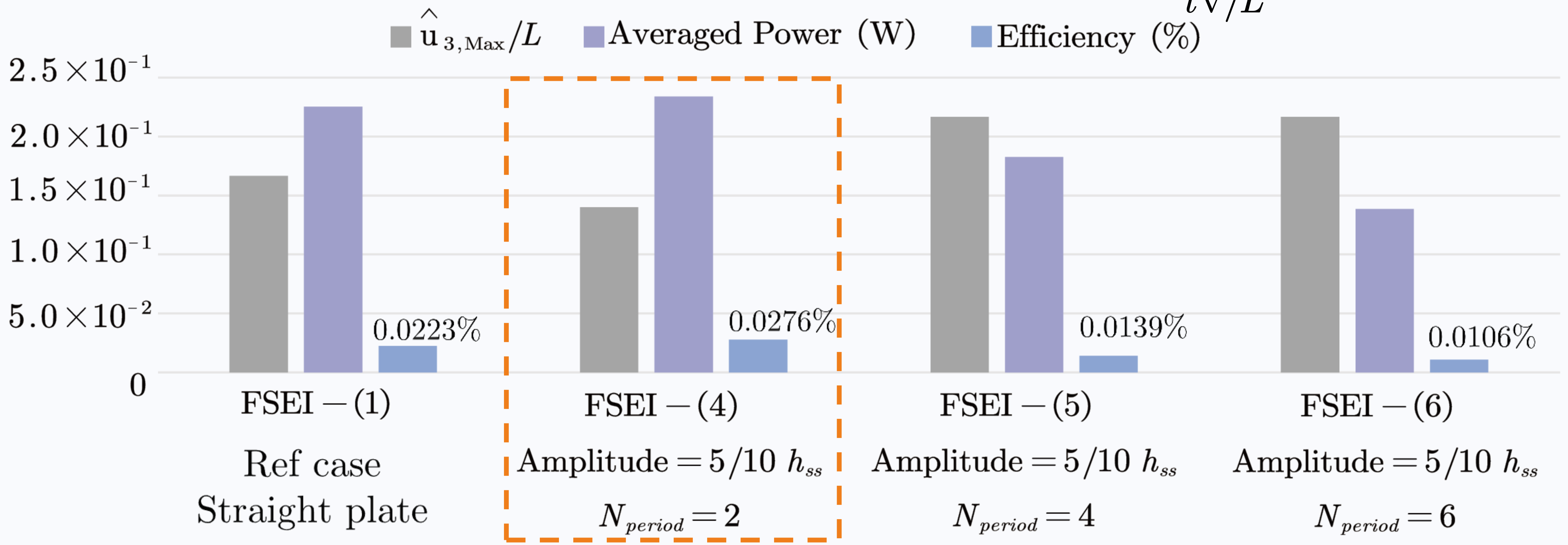

Statistic data extracted from Time history results

- Although $\boldsymbol{N_{period}=4}$ has largest peak power, $\boldsymbol{N_{period}=2}$ reaches the highest efficiency because it has smallest free end displacement and highest averaged power

3. Simulation results

3.3 Cases changing piezoelectric patch

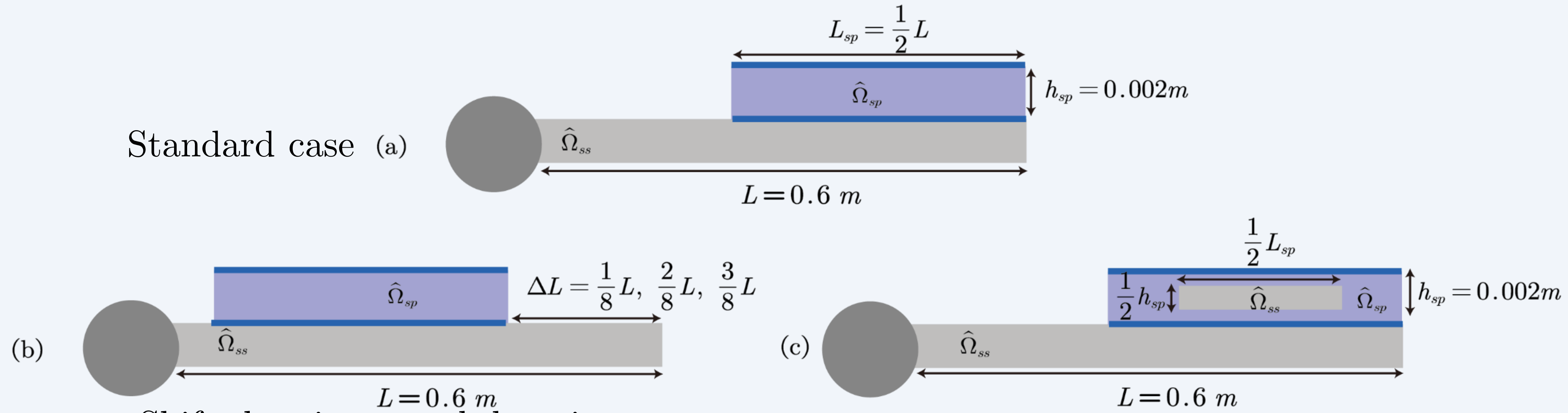

Shift the piezo patch location

With internal inclusion

Cases settings

Case name	$\Delta L / L$	with inclusion in $\widehat{\Omega}_{sp}$
FSEI-(1)	0	no
FSEI-(7)	1/8	no
FSEI-(8)	2/8	no
FSEI-(9)	3/8	no
FSEI-(10)	0	yes

Different location $\begin{cases} \text{FSEI-(1)} \\ \text{FSEI-(7)} \\ \text{FSEI-(8)} \\ \text{FSEI-(9)} \end{cases}$

Inclusion $\begin{cases} \text{FSEI-(1)} \\ \text{FSEI-(10)} \end{cases}$

3. Simulation results

3.3 Cases changing piezoelectric patch - location

Full-body response of the base plate over a complete oscillation cycle

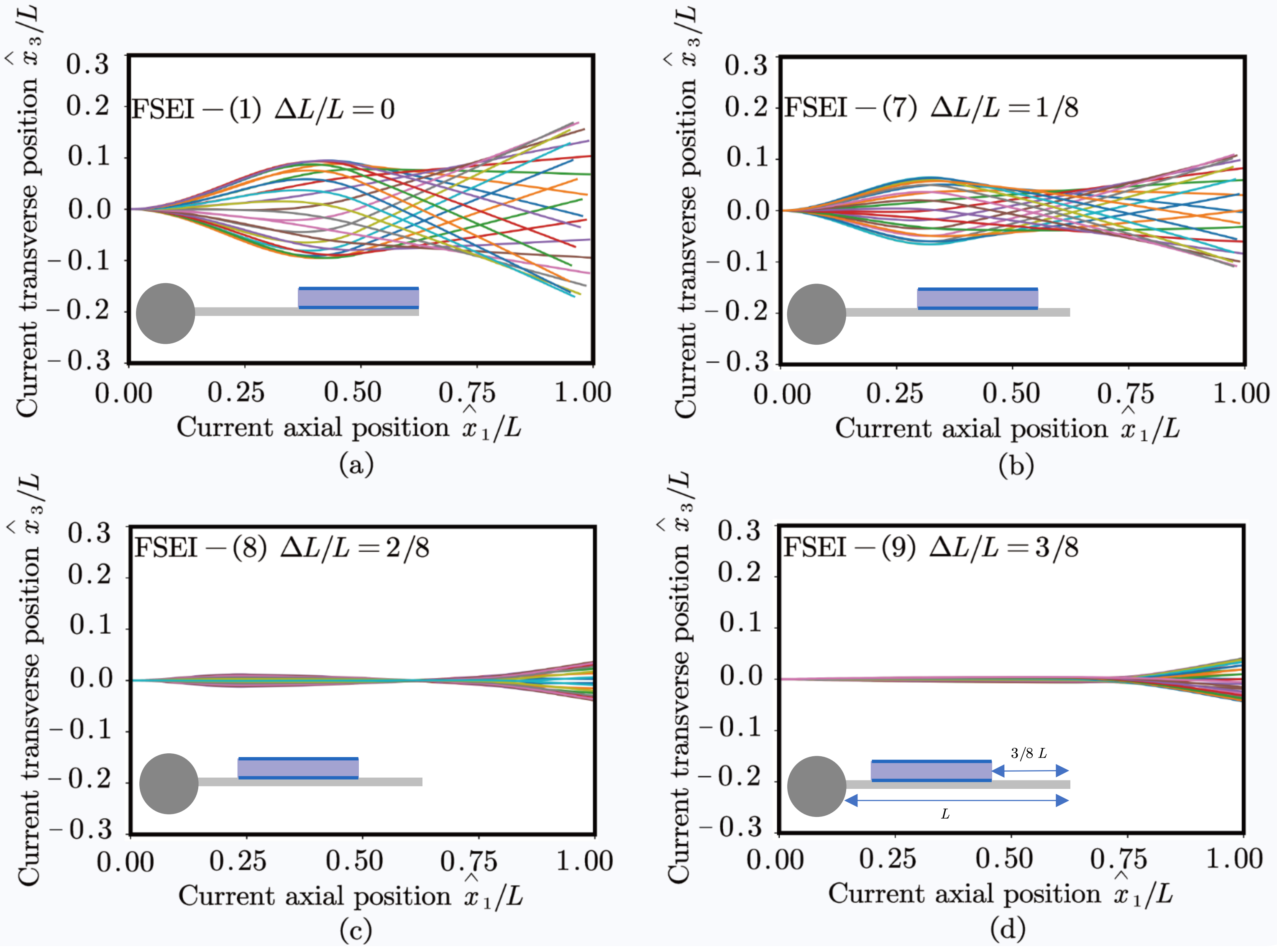

Vortex contours at peak displacement

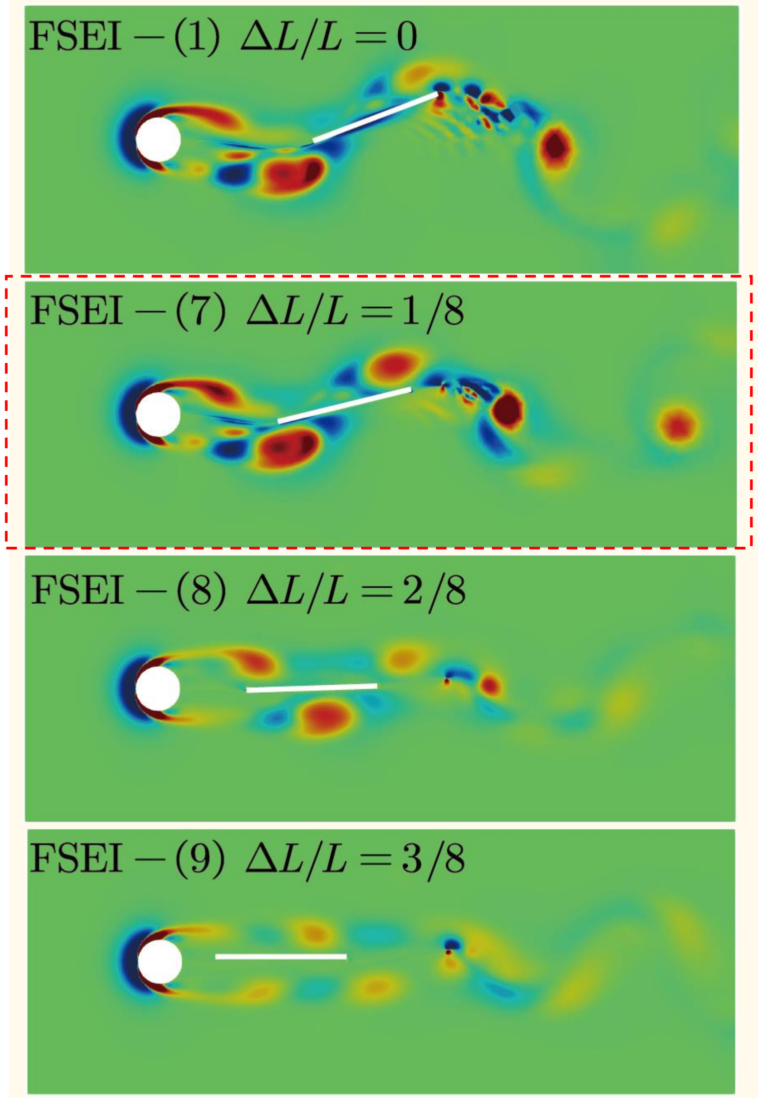

3. Simulation results

3.3 Cases changing piezoelectric patch - location

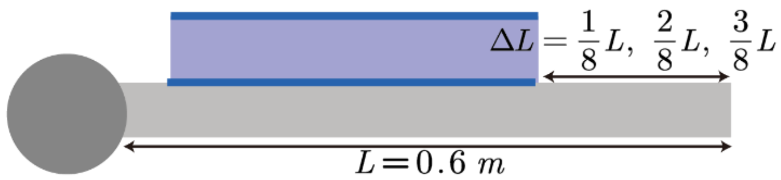

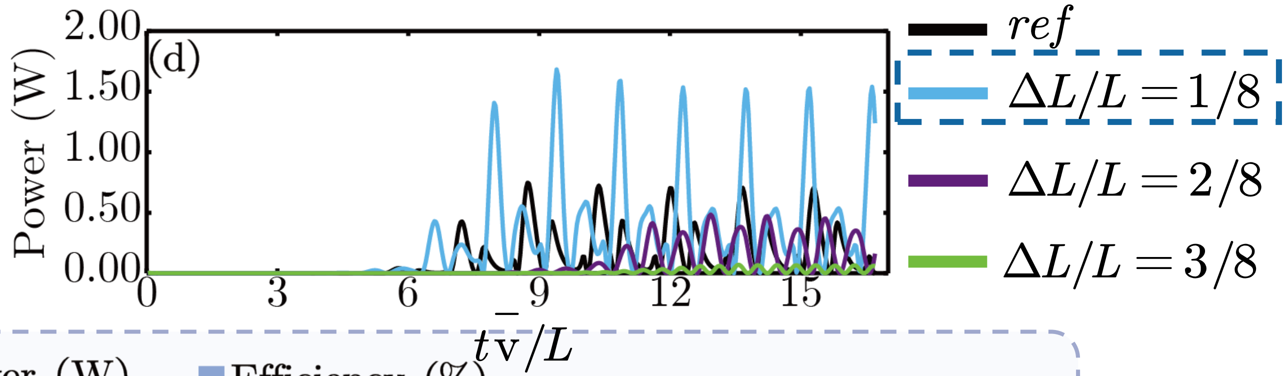

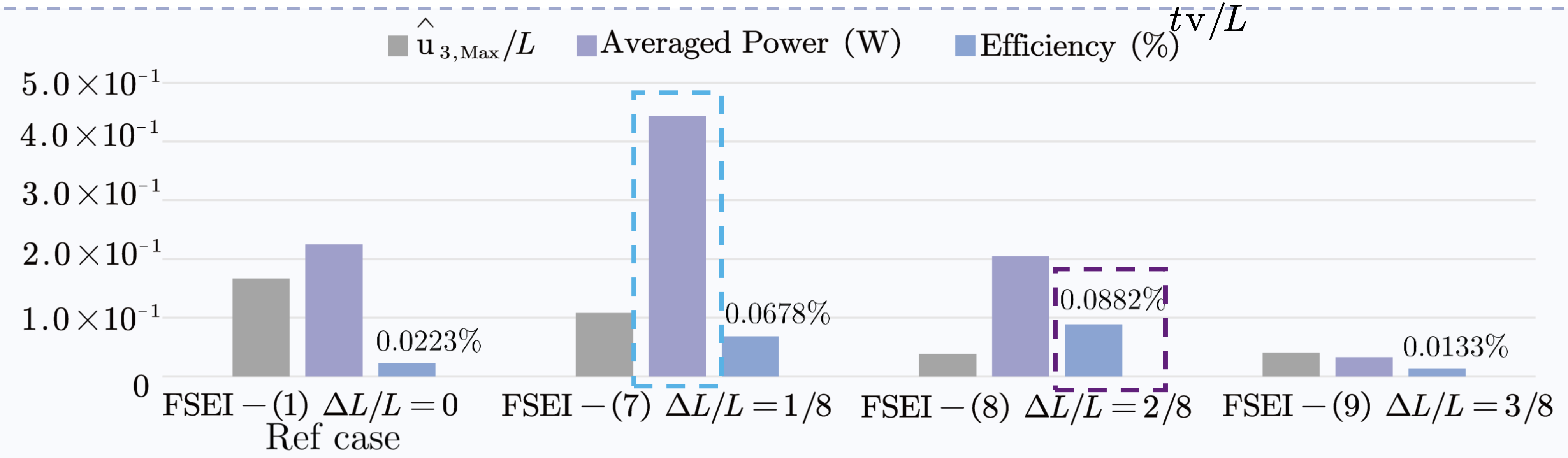

Statistic data extracted from Time history results

- FSEI-(7) gets the highest power, but FSEI-(8) has higher efficiency because of its small free end displacement.
  $\Delta L/L = 1/8$ $\Delta L/L = 2/8$

3. Simulation results

3.3 Cases changing piezoelectric patch – with internal inclusion

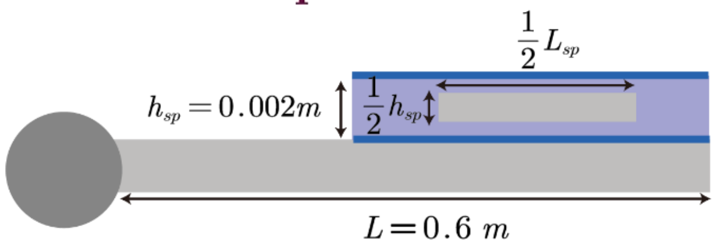

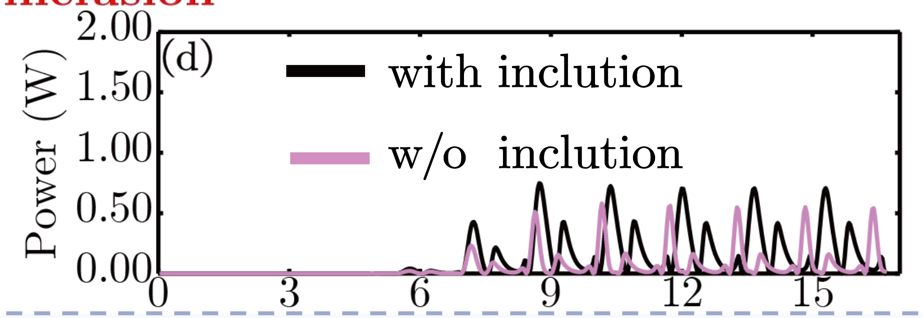

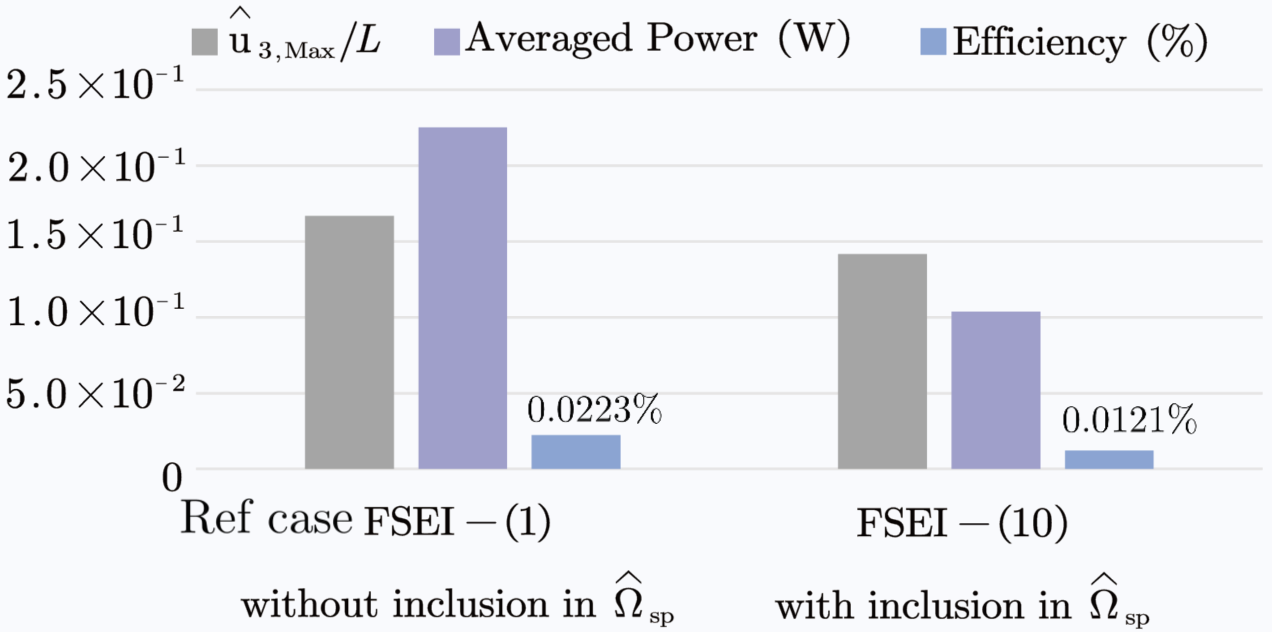

Statistic date extracted from Time history results

- The averaged power has decreased by nearly 53% compared to the standard case, because part of the piezo material is replaced.

04 Model application

A synergistic vortex generator for enhancing PFEH

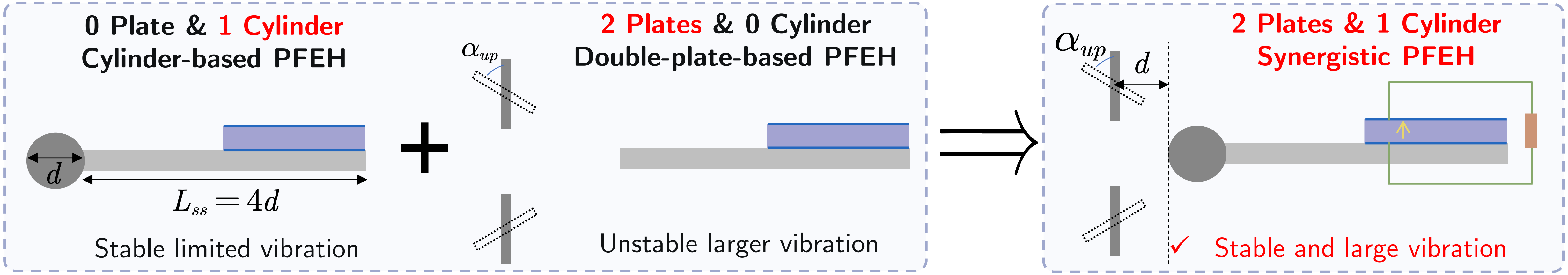

4.1 Cases settings

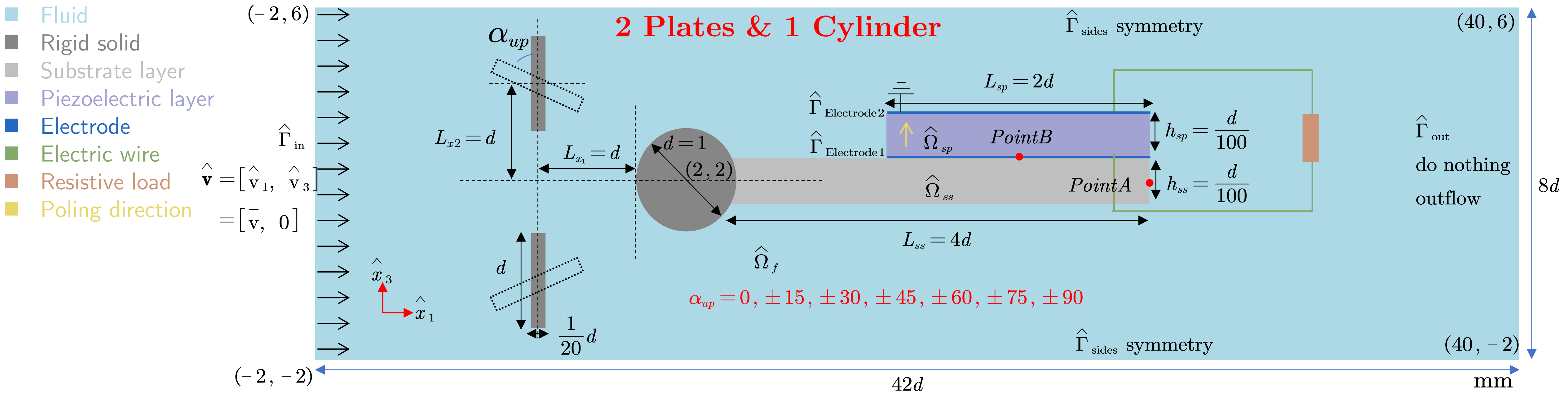

Fluid parameters in $\hat{\Omega}_f$ (Water)

$$\rho_f = 1000 \text{ kg/m}^3$$
$$\mu_f = 0.001 \text{ kg/ms}$$
$$\bar{v}_{inlet} = 0.17 \text{ m/s}$$
$$\text{Re} = \rho_f \bar{v} d / \mu_f = 170$$

Mechanical parameters in $\hat{\Omega}_{ss}$ (Aluminum alloy)

$$\rho_{ss} = 2800 \text{ kg/m}^3$$
$$c_{11} = 112 \text{ GPa}$$
$$c_{12} = 60.5 \text{ GPa}$$

Mechanical and electrical parameters in $\hat{\Omega}_{sp}$ (PZT-5A)

$$\rho_{sp} = 7750 \text{ kg/m}^3$$
$$c_{11} = 120.35 \text{ GPa}$$
$$c_{13} = 75.09 \text{ GPa}$$
$$c_{33} = 110.9 \text{ GPa}$$
$$c_{44} = 21.05 \text{ GPa}$$
$$e_{15} = 12.29 \text{ C} \cdot \text{m}^{-2}$$
$$e_{31} = -5.35 \text{ C} \cdot \text{m}^{-2}$$
$$e_{33} = 15.78 \text{ C} \cdot \text{m}^{-2}$$
$$\epsilon_{11} = 8.14 \times 10^{-9} \text{ C} \cdot \text{V}^{-1}$$
$$\epsilon_{33} = 7.32 \times 10^{-9} \text{ C} \cdot \text{V}^{-1}$$
$$R = 5 \times 10^4 \ \Omega$$

4.2 Cases results - 2Plate & 1Cylinder

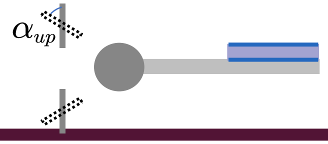

Velocity

Wake forms can be divided into two types

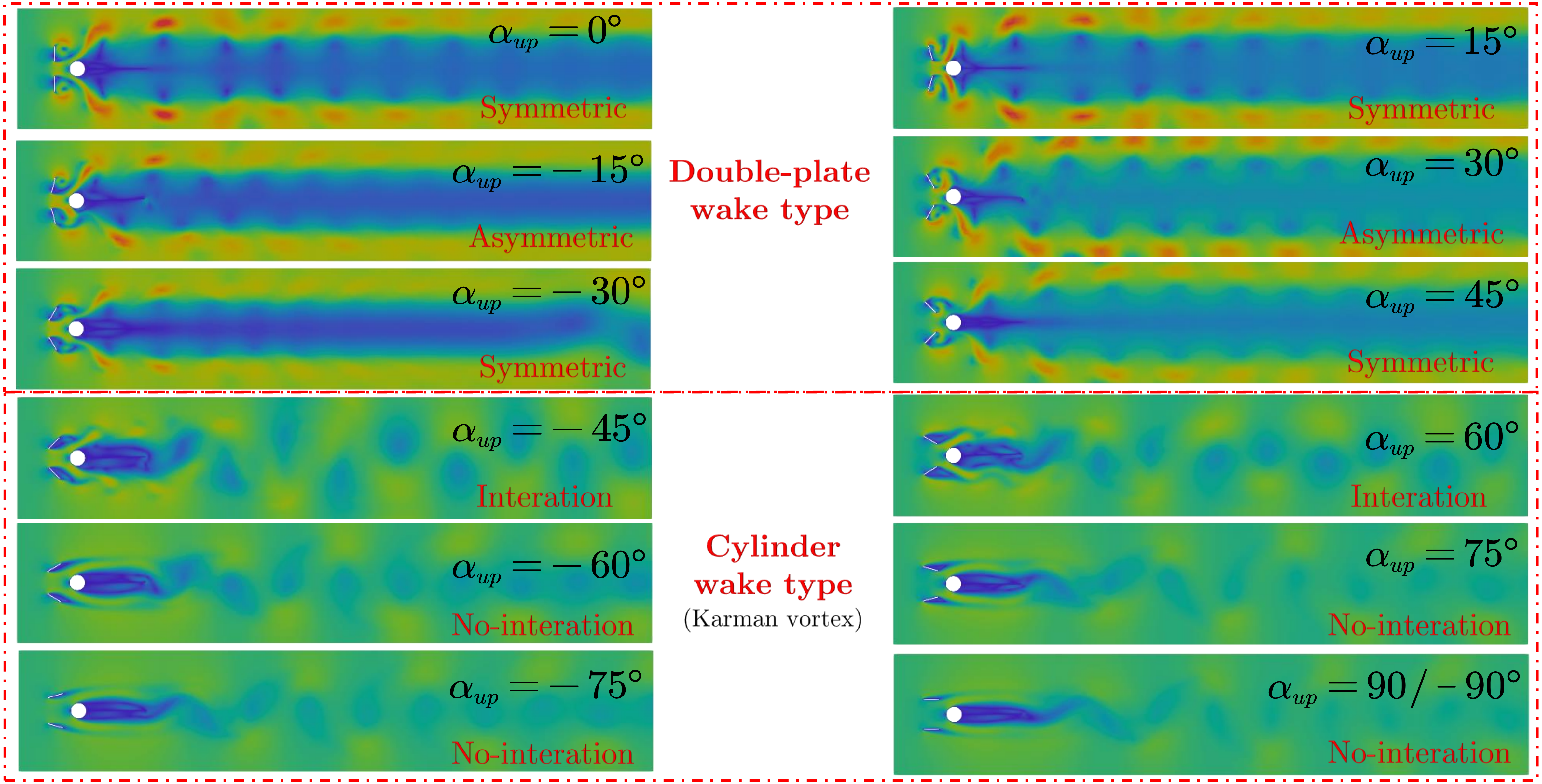

4.2 Cases results - 2Plate & 1Cylinder

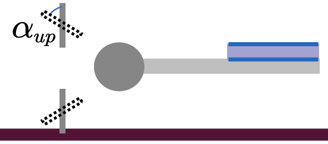

Small angles

$-30° \leqslant \alpha_{up} \leqslant 45°$

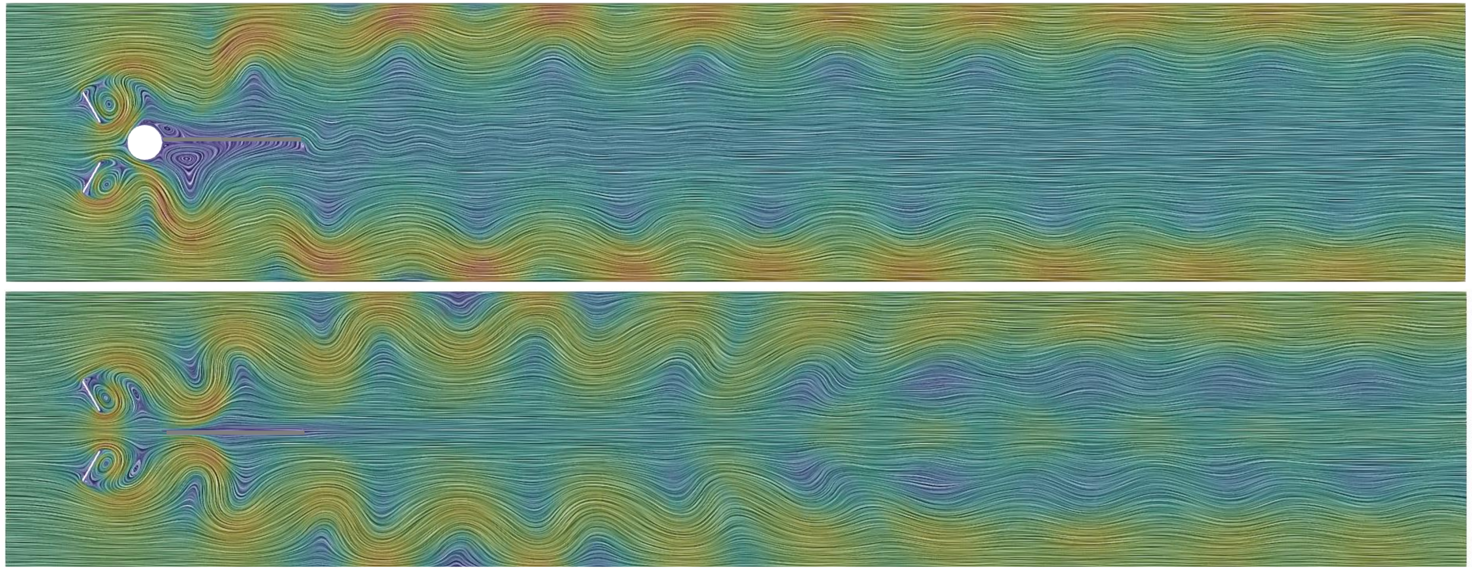

- The Synergistic form will inherit the double-plate wake characteristic.

Large angles

$\alpha_{up} \leqslant -45°$

$\alpha_{up} \geqslant 60°$

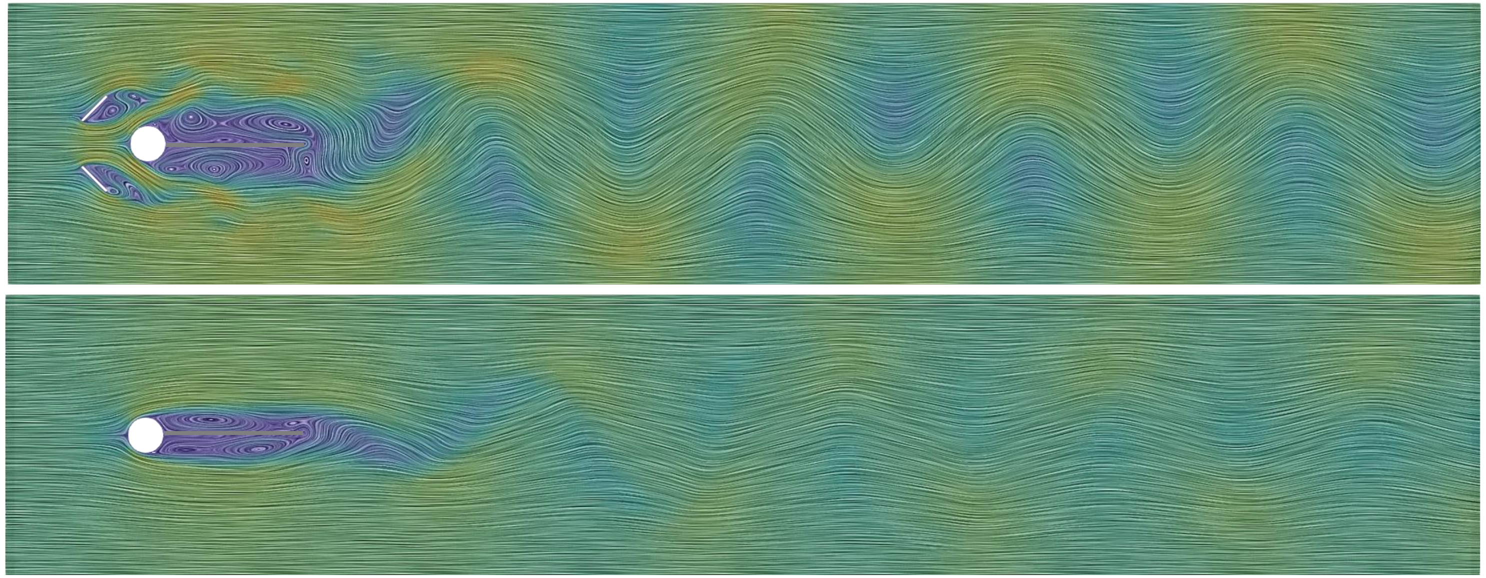

- The Synergistic form will inherit the cylinder wake characteristic.

4.2 Cases results - 2Plate & 1Cylinder

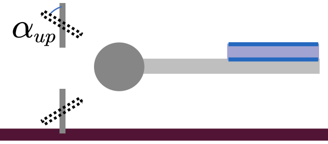

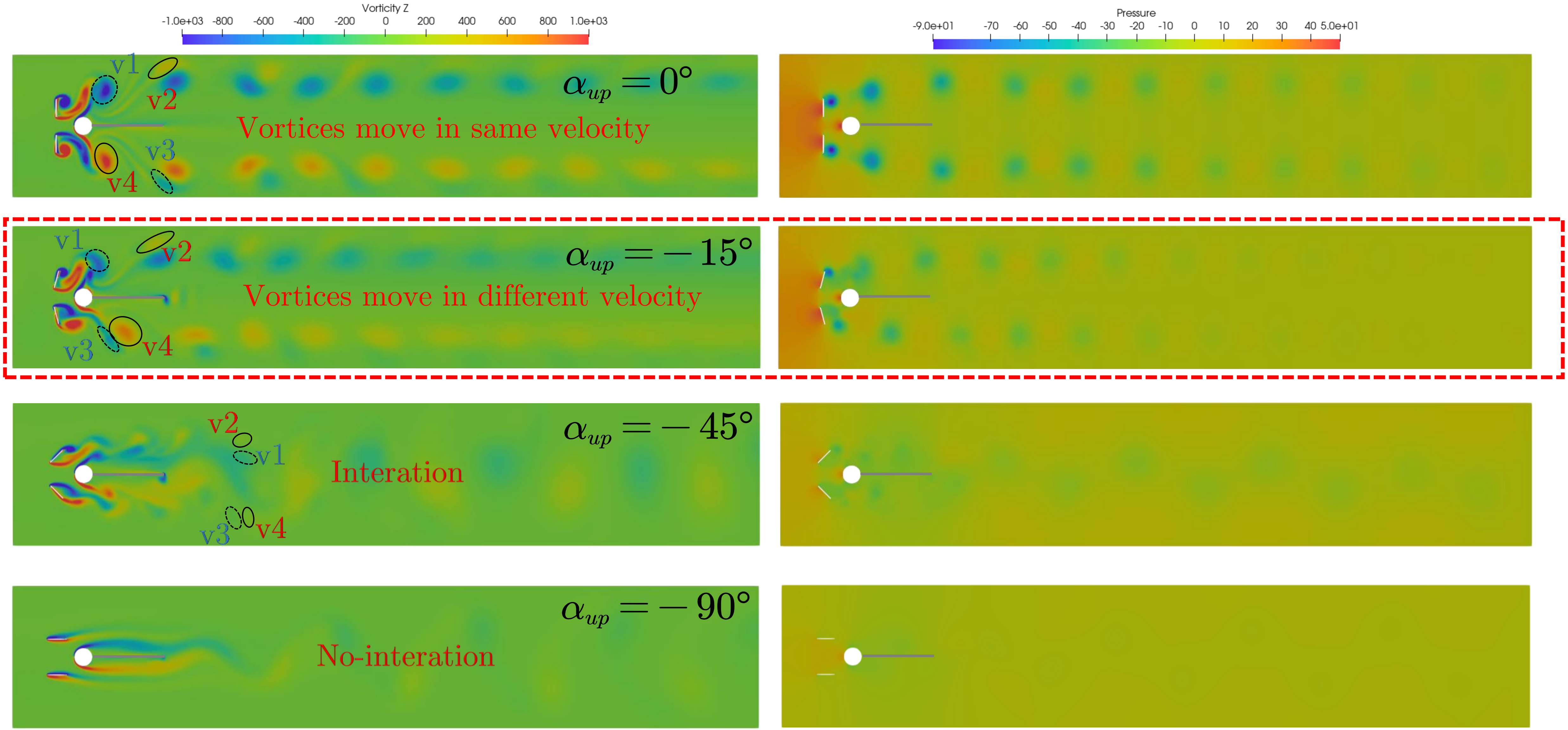

- The asymmetric double-plate wake type is more preferable because it can generate larger pressure difference.

4.2 Cases results - 2Plate & 1Cylinder

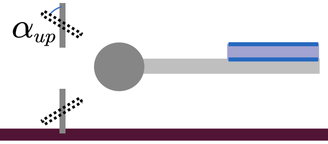

Time history result

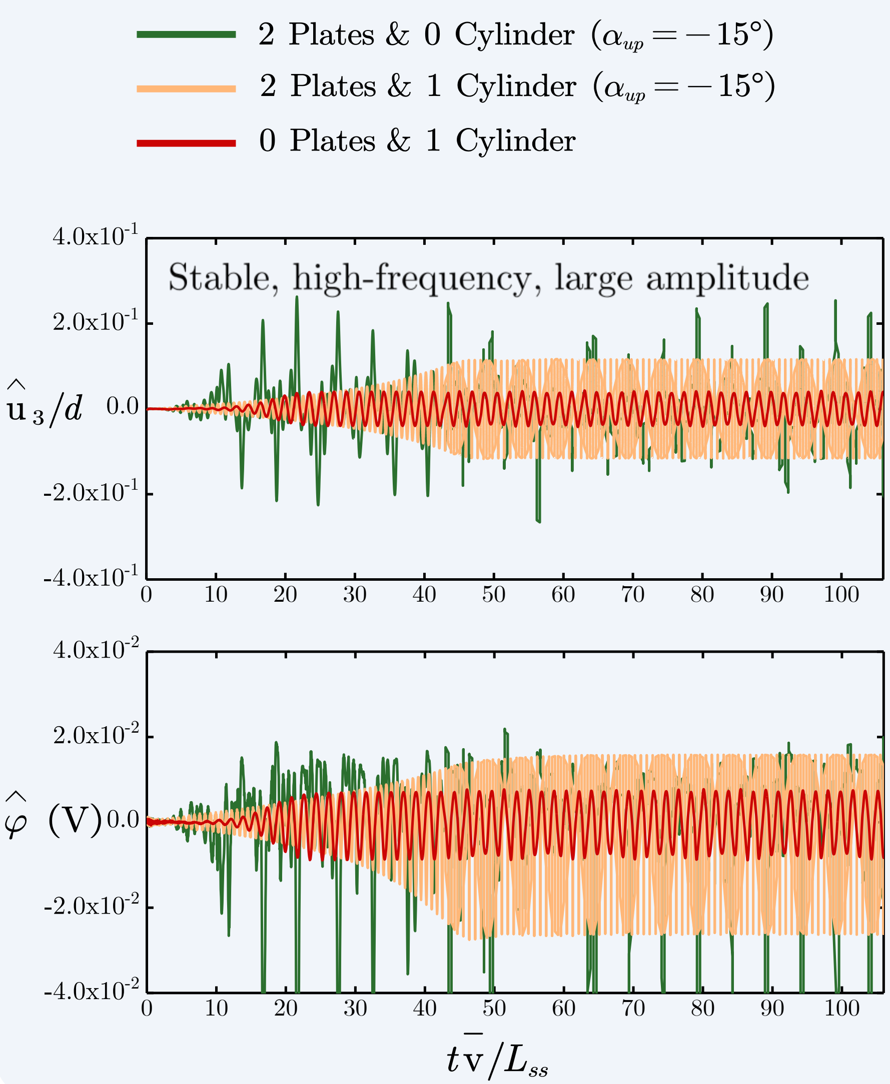

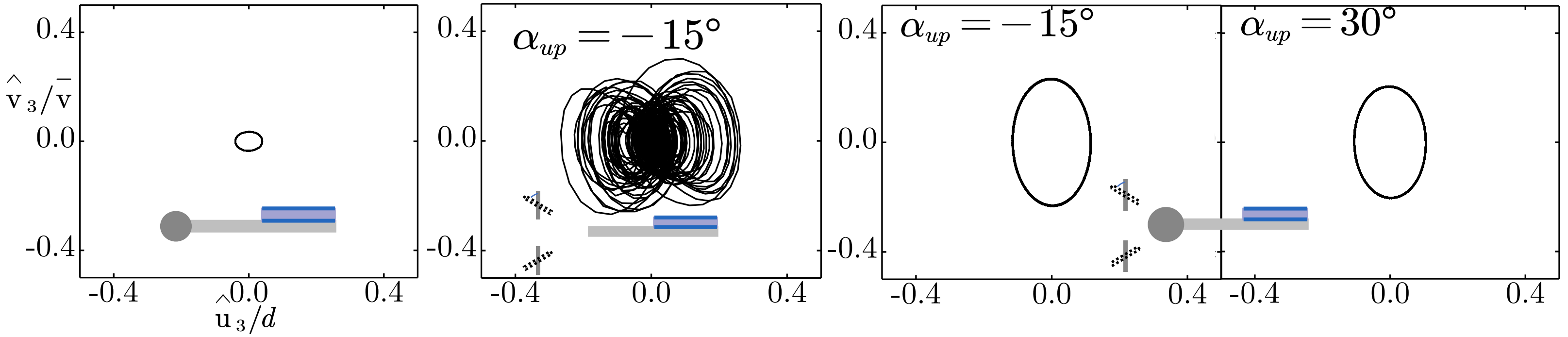

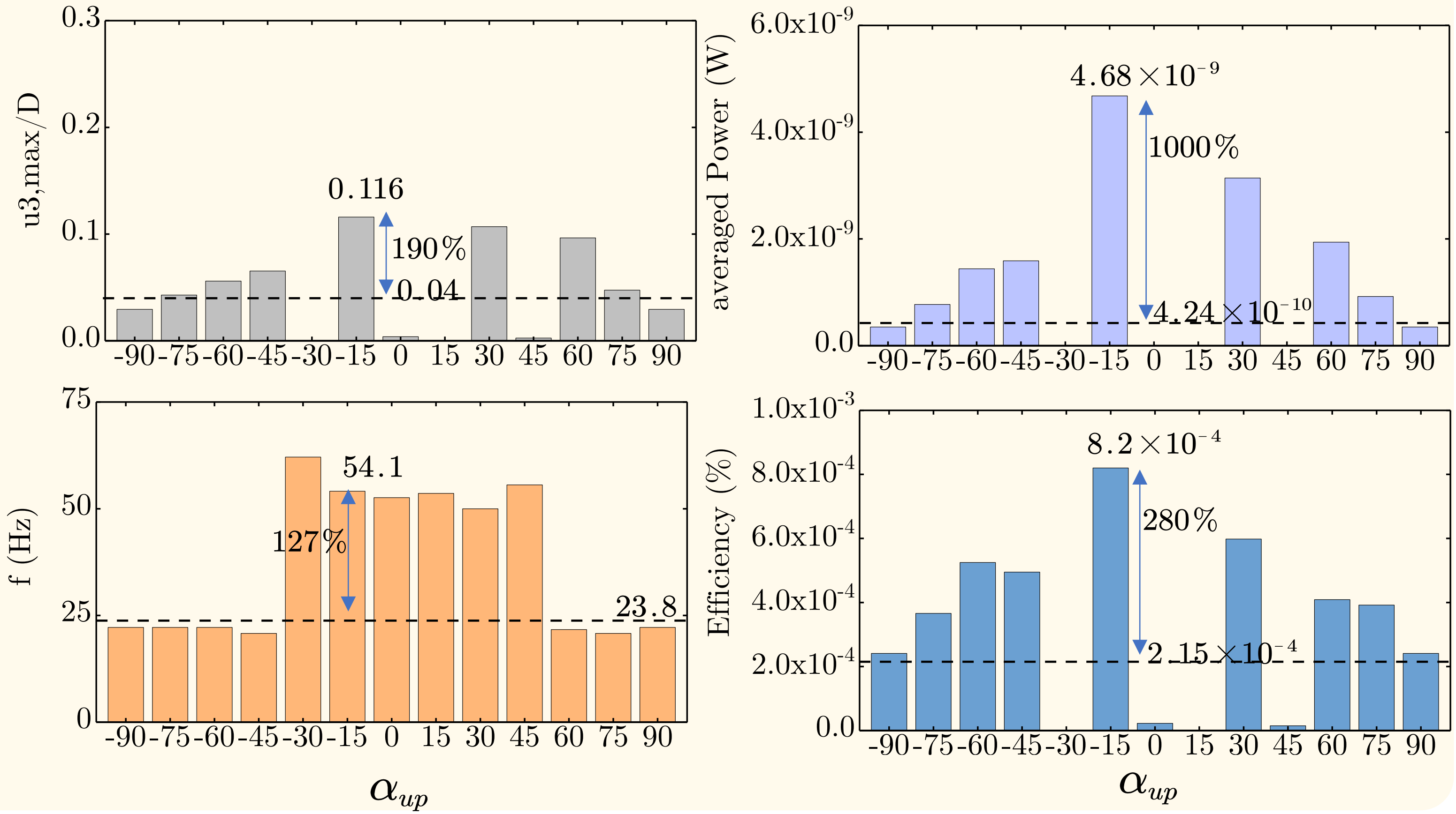

05 Conclusion

5. Conclusion and Future works

Highlights

1. This study introduces a full-scale finite element model for monolithic FSI simulations of thin-walled piezoelectric fluid energy harvesters.
2. The designs of base plate and piezoelectric components have noticeable effects to the dynamic response and electricity outputs of energy harvesters.
3. A synergistic vortex generator is presented for significantly enhancing the PFEH

Future works

1. This model will be extended to 3-Dimentional problems for more detailed designs.
2. Turbulent models will be implemented for applications to high Reynold number conditions.

Thanks for your attention!

Reporter Runze ZHANG

Supervisor A/Prof. Yu CONG